

The Mouse Echocardiography Guide

I. Mouse Heart Anatomy

The mouse heart is about the same size as a pencil eraser, typically weighing 100–200 mg and beating at 400–600 bpm. Because the murine body is parallel to the ground, the mouse heart does not rest on the diaphragm like the human heart, and it therefore has more room to move around within the pericardial cavity. This results in the murine heart having more of an ellipsoidal (rugby ball) shape.

The heart is internally composed of four chambers and divided by a muscular septum into a right and left side. The two chambers on the right side of the heart [right atrium (RA) and right ventricle (RV)] receive partially deoxygenated blood from the body and distribute it via the main pulmonary artery (MPA) to the lungs for gas exchange. The two chambers on the left side of the heart [left atrium (LA) and left ventricle (LV)] receive oxygen-rich blood from the lungs and pump it out to the body through the aorta. Each atrium serves primarily as a reservoir for blood, with only a small amount of pumping action, which assists with ventricular filling. The RV and LV are the major pumping chambers for providing blood to the pulmonary and systemic circulations, respectively.

There are four valves located within the heart that ensure blood flows in only one direction through it: from the atrium to the ventricle and out through its appropriate artery. The two atrioventricular (AV) valves are located between the atrium and ventricle on both the left and right sides of the heart. Lying between the RA and RV is the right AV valve; the left AV valve lies between the LA and LV. The right AV valve [or tricuspid valve (TV)] has three distinct leaflets, whereas the left AV valve [also known as the mitral valve (MV) or bicuspid valve] has two distinct leaflets.

The primary function of the two AV valves is to prevent the blood from the ventricles regurgitating to the atrium during ventricular systolic contraction and thereby ensuring unidirectional flow. Blood flows from the veins into the RA and passes through the TV into the RV. Contraction of the RV sends the blood through the pulmonary valve toward the lungs. As the RV contracts the TV closes so as to prevent regurgitation of blood back into the RA. The closing of the TV and the other one-way valves creates the heartbeat sound.

The two other valves within the heart are (1) the pulmonary valve, located at the junction of the RV and MPA, and (2) the aortic valve that lies at the junction of the LV and the aorta. These two valves are sometimes referred to as semilunar valves because they consist of three half-moon-shaped valve cusps. The function of the semilunar valves is to prevent regurgitation of blood from the MPA and aorta back into the ventricles when the ventricles relax following contraction. [1]

The striking feature of the mouse heart and vessels that differs from other species is the arrangement of the coronary venous system. The cardiac veins are the most prominent structures on the epicardial surface of the LV, far exceeding the visibility of the coronary arteries. Small cardiac veins are at approximate right angles to the largest coronary vein, the left cardiac vein, which proceeds to the ventral surface of the LV and the apex of the heart toward the dorsum of the heart to drain into the left anterior vena cava at its junction with the right anterior and posterior vena cava connection with the RA. In addition, there are two major veins that drain the

conal region of the RV and the ventrocephalic region of the LV. These are called the extracoronary cardiac veins because they originate at the heart and terminate in vessels not otherwise associated with the coronary circulation—in this case the anterior vena cava.

The heart muscle receives a rich blood supply from the coronary arteries that branch from the aorta. Observing the coronary artery system of the mouse heart is much more difficult than observing the coronary venous system—a source of intense light and magnification is required to visualize these deeper and more hidden vessels. The right coronary artery usually divides into two major branches: one supplying the RV and the other the septal region. The left coronary artery (LCA) generally divides into a major septal branch and the left anterior descending coronary artery supplying the free wall of the LV, part of the septum, and the apical region of the LV. The left circumflex coronary artery, which is a major branch of the LCA in other animal species and humans, is not clearly a major vessel in mice, appearing instead as a rudimentary structure. Therefore, the variability in epicardial coronary architecture is a very important consideration even in the same genetic stock. [2]

II. The Mouse Orientation and its Spatial Relation to the Ultrasound Transducer

In mice, the postero-inferior location of the lung lobes relative to heart, the narrow sternum, and the relative large thymus (which is hypoechoic in ultrasound imaging) results in large parasternal acoustic windows on both the right and left sides of the sternum during transthoracic cardiac imaging [3]. The terms “superior”, “inferior”, “anterior”, and “posterior” are used to define the transducer orientation relative to the mouse, which correspond to the cranial, caudal, ventral, and dorsal aspects of the mouse’s body, respectively [Fig. 1(A)]. Using the transducer to scan the mouse in any plane will produce the two-dimensional image for that plane. The central axis of the transducer provides the basic guideline for the imaging direction, as shown in Fig. 1(B).

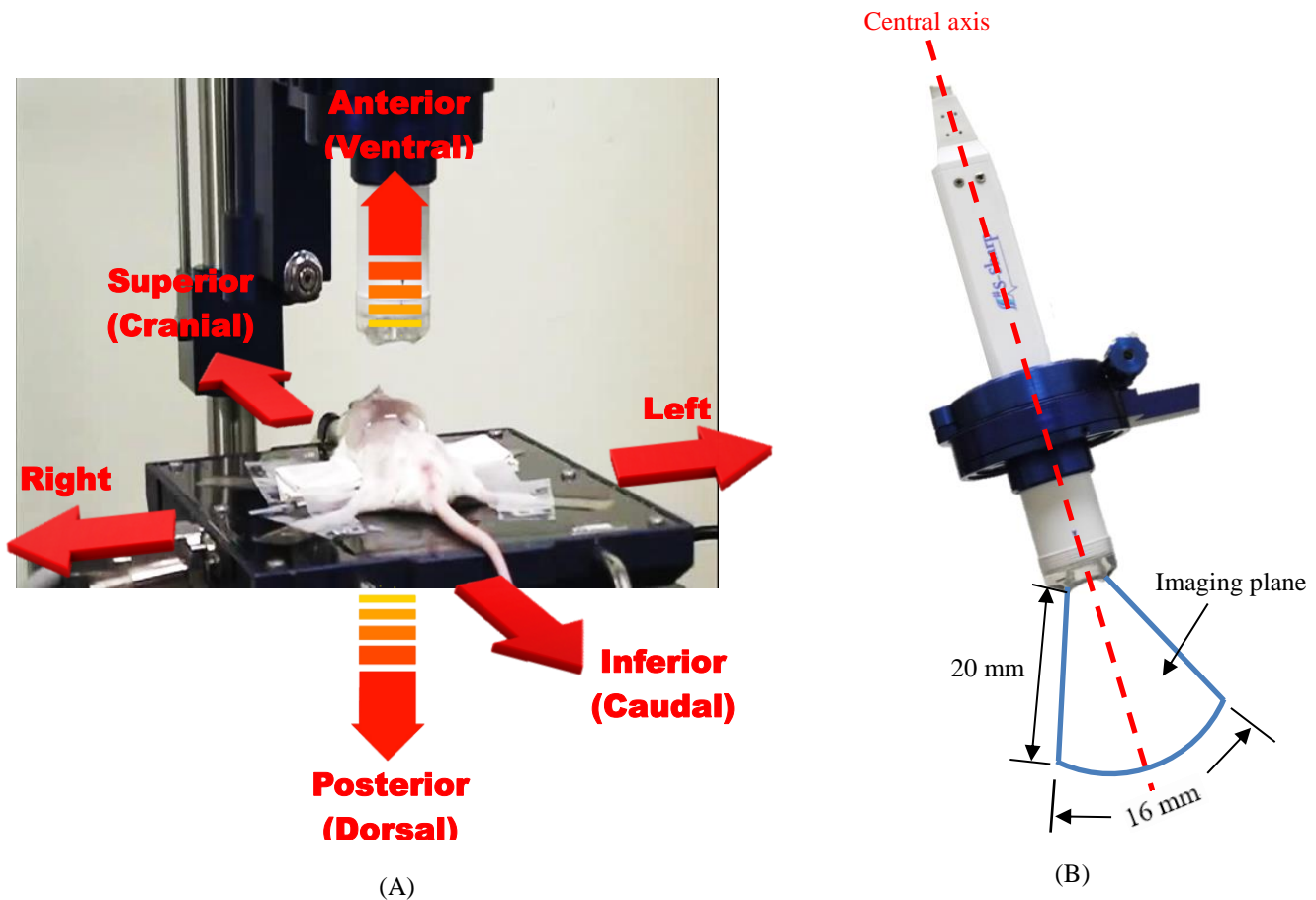


Fig. 1. (A) The mouse orientation and its spatial relation to the transducer. (B) Configuration of two-dimensional imaging plane and the central axis of the transducer.

N.B. The starting position of the scan is indicated by a red dot in all of the following figures showing configurations, and the corresponding imaging is started from the left-most position of the image.

The Table 1 lists the acronyms used in this document:

Table 1. The acronyms used in this document

| Acronym | Full term | Acronym | Full term |
|----------------|-------------------------|----------------|--|
| AAo | ascending aorta | TV | tricuspid valve |
| AAr | aortic arch | Th | thymus |
| AO | aortic orifice | LVAW / LVPW | left ventricular anterior wall / left ventricular posterior wall |
| AV | atrioventricular | LA / RA | left atrium / right atrium |
| IA | innominate artery | LV / RV | left ventricle / right ventricle |
| IVS | interventricular septum | LCCA / RCCA | left common carotid artery / right common carotid artery |
| LCA | left coronary artery | LSCA / RSCA | left subclavian artery / right subclavian artery |
| MPA | main pulmonary artery | LSVC / RSVC | left superior vena cava / right superior vena cava |
| MV | mitral valve | LVIT | left ventricular inflow tract |
| PM | papillary muscle | LVOT / RVOT | left ventricular outflow tract / right ventricular outflow tract |
| PO | pulmonary orifice | RPV/RPA | right pulmonary vein / right pulmonary artery |

Also, all of the representative targeted structures of transthoracic cardiac imaging in this guide, imaging sections, applied ultrasound imaging modalities, and measurements are summarized in the Table 2:

Table 2. Summary of the representation sections, imaging modalities, and measurements of all targeted structures in mice

| Targeted structures/views | Imaging sections | Imaging modalities | Measurements |
|----------------------------------|---|---------------------------|--|
| RSVC | Right paraternal longitudinal section | B/PW-mode | Doppler flow spectrum |
| RPV | Left paraternal longitudinal section | B/PW-mode | Doppler flow spectrum |
| TV | Right parasternal transverse section/ apical four-chamber view | B/PW-mode | Doppler flow spectrum |
| MV | Right parasternal longitudinal section/ apical four-chamber view | B/M/PW-mode | Movement of the MV's anterior leaflet/ Doppler flow spectrum |
| Long-Axis view | Left parasternal longitudinal section | B/M-mode | **LVmass/TVS(d,s)/LVID(d,s)/LV vol(d,s)/LVPW(d,s)/LVEF/LVFS/SV/ CO |
| Short-Axis view | Left parasternal transverse section | B/M-mode | **LVmass/LVAW(d,s)/ LVID(d,s)/LVPW(d,s)/LVEF/LV vol(d,s)/LVFS/SV/CO |
| MPA | Left parasternal longitudinal section | B/PW-mode | Maximum blood velocity of MPA |
| RVOT | Left parasternal longitudinal section | B/M-mode | Dimension changes of RVOT, AAo, and RA |
| AO/AAo | Upper right parasternal longitudinal section/ lower right parasternal longitudinal section | B/M/PW-mode | AO diameter/movement of the aortic cusps/dimension changes of the AAo/maximum blood velocity in AAo |
| LCA | Left parasternal transverse section | B/PW-mode | Doppler flow spectrum |
| AAr | Right parasternal longitudinal section | B-mode | |
| RCCA | Right parasternal longitudinal section | B-mode | |

** LVmass, left ventricular mass; LVAW(d,s), left ventricular anterior wall diastolic or systolic dimension; IVS(d,s), interventricular septum diastolic or systolic dimension; left ventricle internal diastolic or systolic dimension; LVPW(d,s), left ventricular posterior wall diastolic or systolic dimension; LVEF, left ventricular ejection fraction; LVFS, left ventricular fraction shortening; SV, stroke volume; CO, cardiac output.

III. Transducer Position and Sonography Procedures

A. Right Superior Vena Cava

The right superior vena cava (RSVC) is one of the RA inflow channels. It is most readily visualized from a right parasternal longitudinal section in the B-mode image, for which the long hinge of platform should be initially moved clockwise by $30^{\circ}\sim 60^{\circ}$ from the anterior view, and the short hinge of platform should be displaced counterclockwise by $0\sim 10^{\circ}$ from the inferior view, and moved close to the surface toward the more posterior section of the mouse. The transducer should then be parallel to the central axis of the mouse, aimed at the upper one-third of the chest, as shown in Fig. 2. Finally, the platform should be set so the longitudinal section of the RSVC can be displayed. PW-mode (pulsed-wave Doppler mode) imaging can be used to estimate the blood velocity in the RSVC and show its Doppler flow spectrum. As indicated in Fig. 3, the Doppler flow spectrum of RSVC shows a small retrograde A wave caused by atrial contraction during late diastole, a medium D wave during early diastole, and a relatively larger S wave during systole. The A wave precedes the S wave, which is followed by the D wave. This pattern is repeated during each cardiac cycle. A dramatic increase in the amplitude and a change in the shape of the waveforms are observed around the end of inspiration. The longitudinal section of the left superior vena cava (LSVC) is in the same position as the RSVC but moved leftward in parallel in the left parasternal longitudinal section.

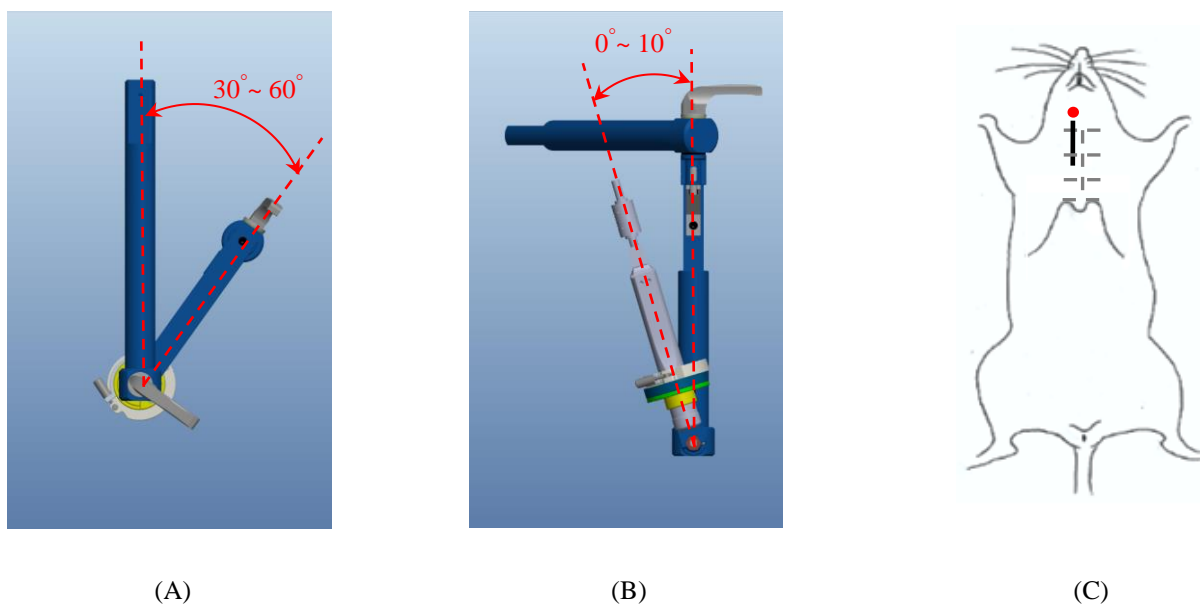
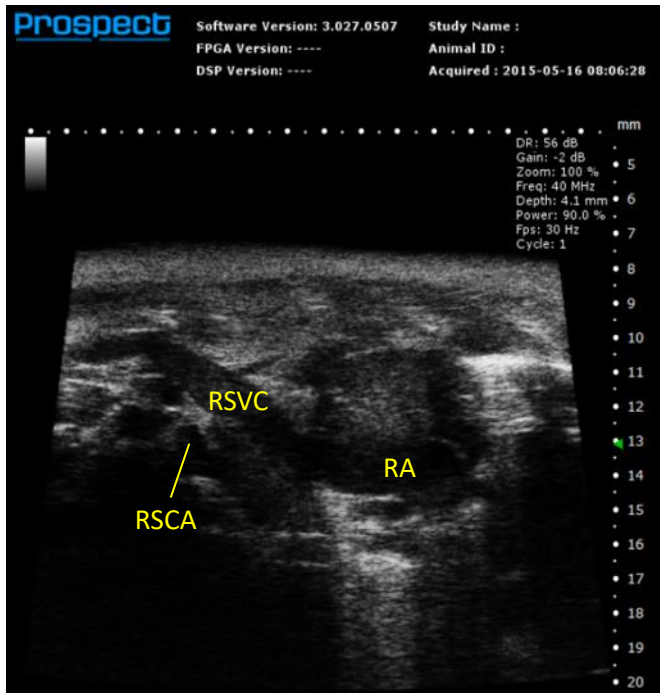
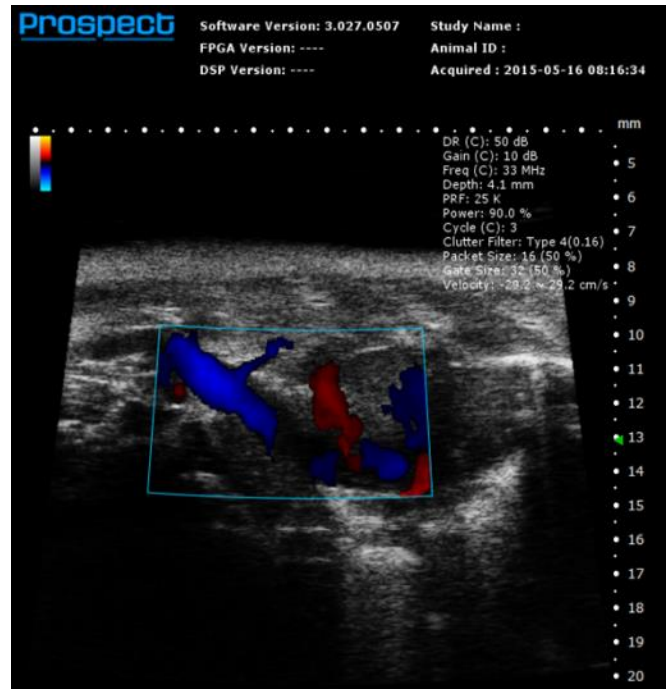


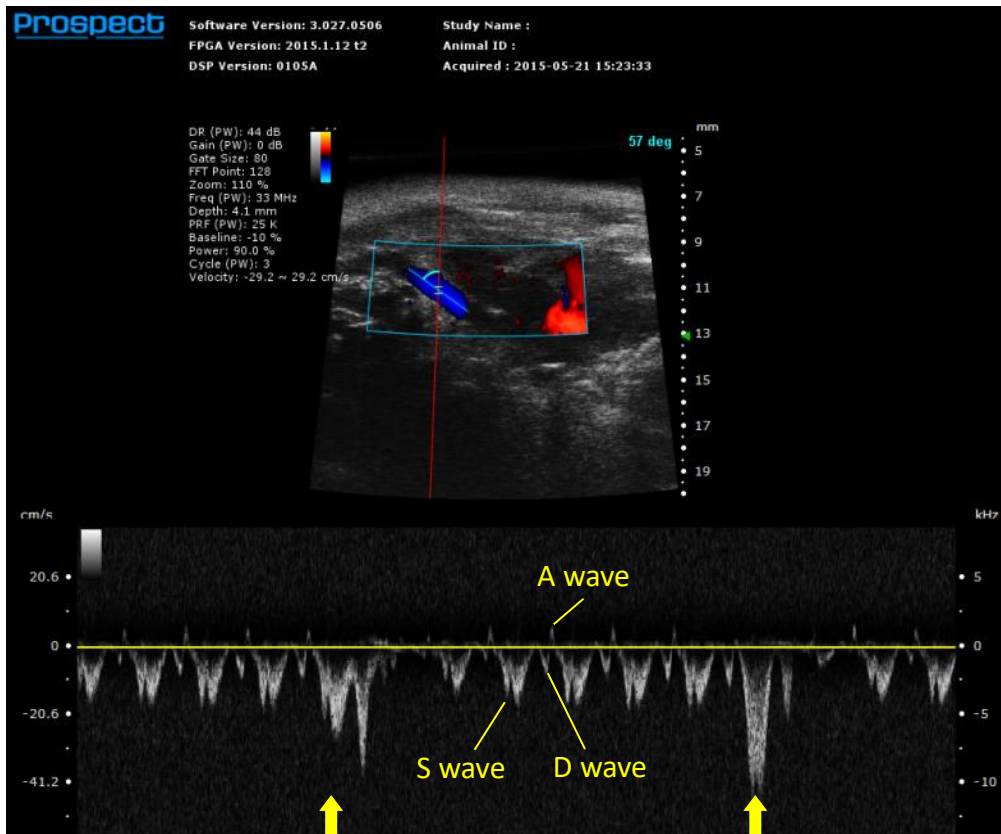
Fig. 2. Configuration of operation showing how to image the right superior vena cava (RSVC) in the right parasternal longitudinal section. (A) Long hinge position from the anterior view. (B) Short hinge position from the inferior view. (C) Transducer position.



(A)



(B)



(C)

Fig. 3. RSVC imaging of the mouse: (A) B-mode image, (B) color Doppler-mode image at its lumen, (C) PW-mode image, and the visualization of the blood flow is provided within the blue rectangle which indicates the region of interest (ROI), and the red line indicates the transmission direction of the pulse wave sent from the transducer. A yellow gate and a cyan line are located on the red line, they indicate Doppler sample volume and Doppler angle respectively and both can be regulated. Arrow indicates a large S wave at the end of inspiration. RA, right atrium; RSCA, right subclavian artery; Th, thymus.

B. Right Pulmonary Vein

The right pulmonary vein (RPV) is the LA inflow channel and is readily visible in the left parasternal longitudinal section in B-mode imaging. To view this the long hinge of platform should be moved clockwise by $60^{\circ}\sim 90^{\circ}$ from the anterior view, and the short hinge of platform should be displayed clockwise or counterclockwise by about 5° from the right side view. At the same time the transducer should be parallel to the central axis of the mouse and positioned at the middle-to-lower one-third of its chest, aimed toward the more posterior section of the mouse, and rotated counterclockwise by about 15° (Fig. 4). Switching to PW-mode imaging will reveal the Doppler flow spectrum and the blood velocity of the RPV. A small retrograde A wave caused by atrial contraction during late diastole, a considerably larger D wave during early diastole, and a smaller S wave during systole with a slight decrease in D wave during inspiration are visible (Fig. 5). The angle between the transducer and the platform can be reduced when necessary to reduce the shadow caused by the mouse sternum.

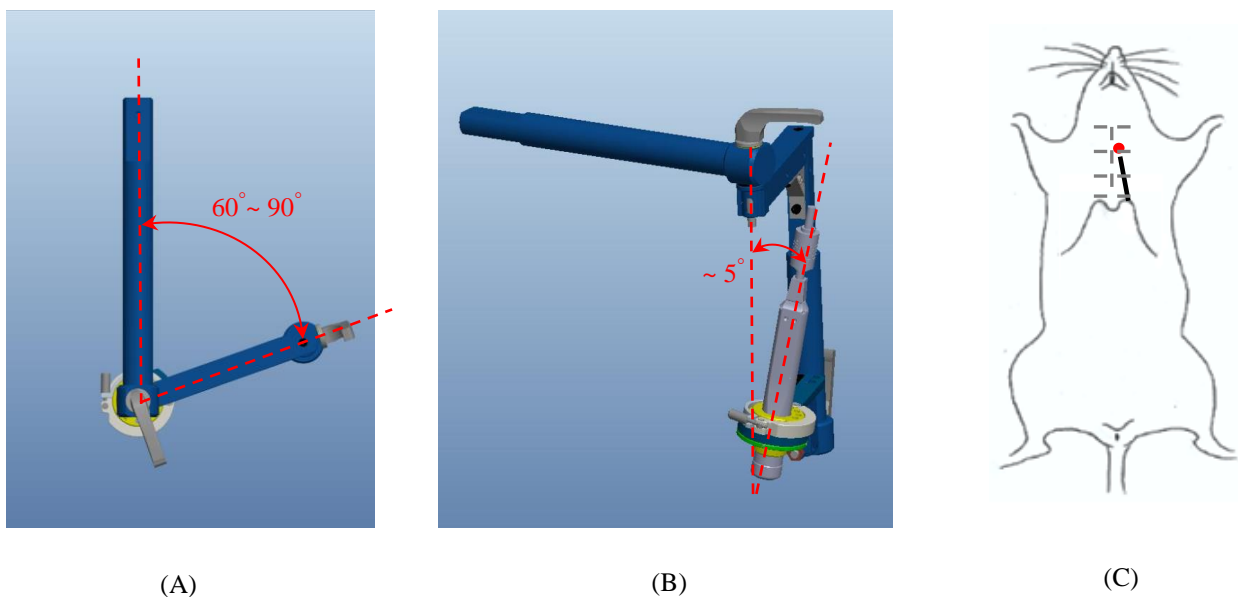
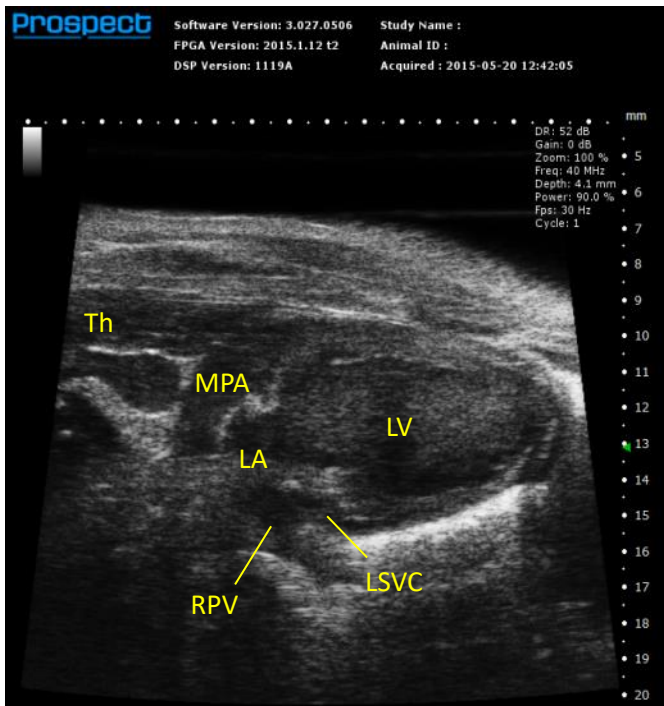
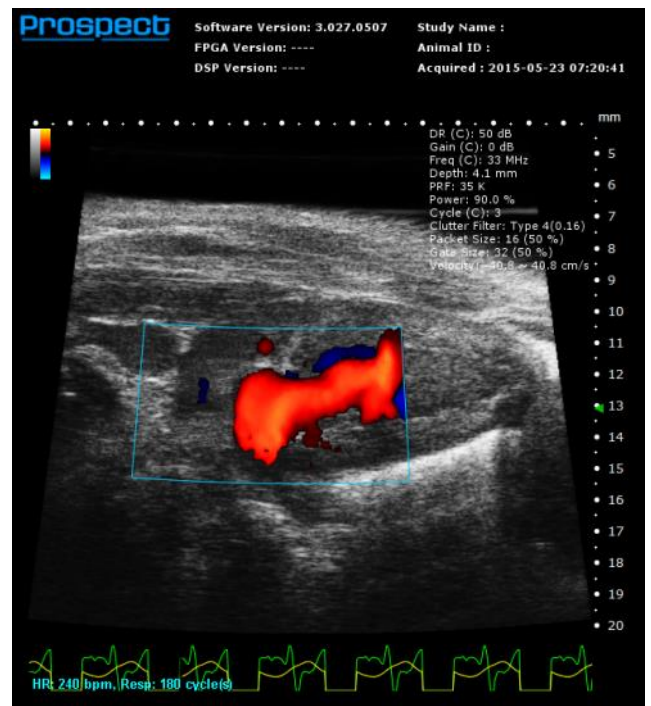


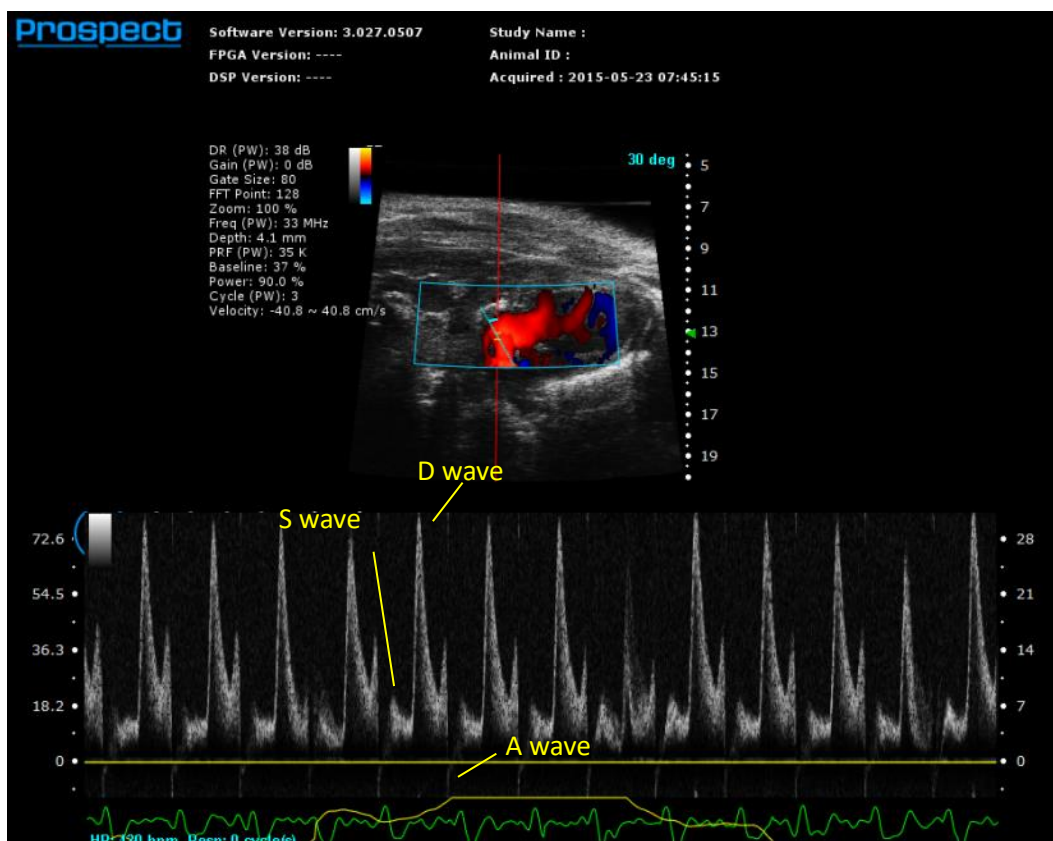
Fig. 4. Configuration of operation showing how to image the right pulmonary vein (RPV) in the left parasternal longitudinal section. (A) Long hinge position from the anterior view. (B) Short hinge position from the inferior view. (C) Transducer position.



(A)



(B)



(C)

Fig. 5. RPV imaging of the mouse: (A) B-mode image, (B) color Doppler-mode image, and (C) PW-mode image at its lumen. LSVC, left superior vena cava; LV, left ventricle.

C. Tricuspid Valve

The TV is located between the RA and RV, and can be viewed in the right parasternal transverse section and the apical four-chamber view. The right parasternal transverse section can be displayed by positioning the long hinge of platform by 0° from the anterior view, and moving the short hinge of platform counterclockwise by $0^\circ\sim 5^\circ$ from the inferior view. The transducer should also be displaced on the lower one-third of the chest, rotated it counterclockwise by about 30° from the plane perpendicular to the central axis of mouse, and moved it close to the surface (Fig. 6). In this view the RA, tricuspid orifice, and RV are visualized in the B-mode image [Fig. 7(A)]. The tricuspid Doppler flow spectrum is readily recorded by using PW-mode imaging, and it shows a smaller early diastolic ventricular filling wave (E wave), a larger late diastolic ventricular filling wave due to the atrial contraction (A wave), and a considerable increase in the amplitude of the waveform during inspiration, as shown in Fig. 7(B) and (C). The apical four-chamber view provides another option for observing the TV. This view can be displayed by adjusting the long hinge of platform clockwise by $60^\circ\sim 90^\circ$ from the anterior view, and moving the short hinge of platform clockwise by $30^\circ\sim 60^\circ$ from the right side view. The transducer should then be moved above the left side of the xiphoid, perpendicular to the central axis of the mouse's body, rotated counterclockwise by about 45° , and aimed at the posterior section of the mouse. Finally, the central axis of the transducer should be aimed at the superior section of the mouse $30^\circ\sim 60^\circ$ from the platform (Fig. 8). In the apical four-chamber view, the LV, LA, RV, RA, MV, and TV can be visualized simultaneously in the B-mode image [Fig. 9(A)]. The tricuspid Doppler flow spectrum can be revealed by switching to PW-mode imaging [Fig. 9(B) and (C)].

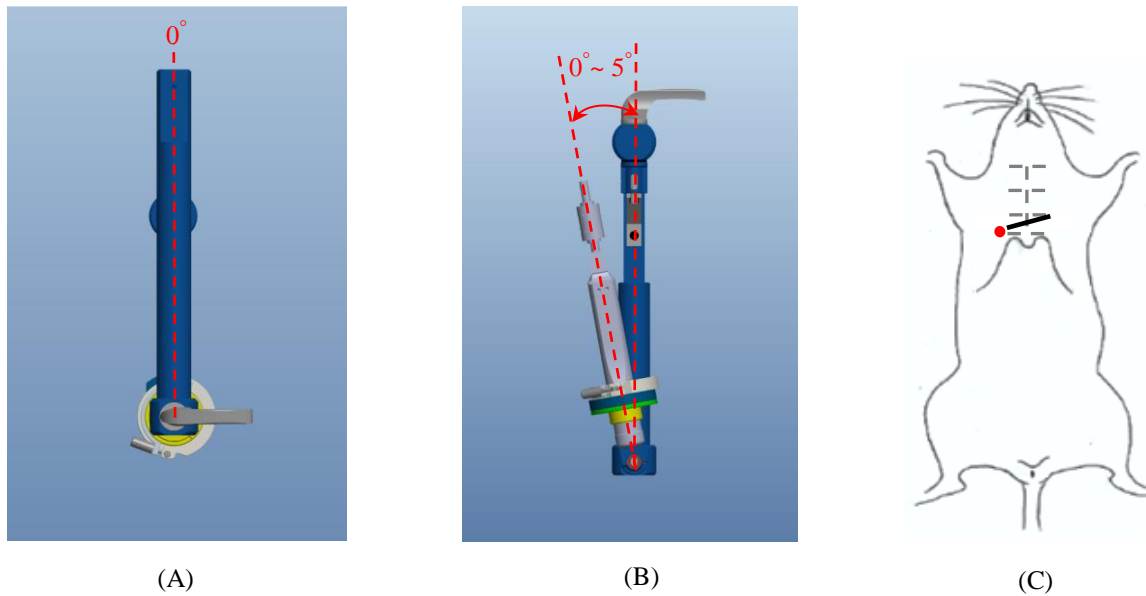
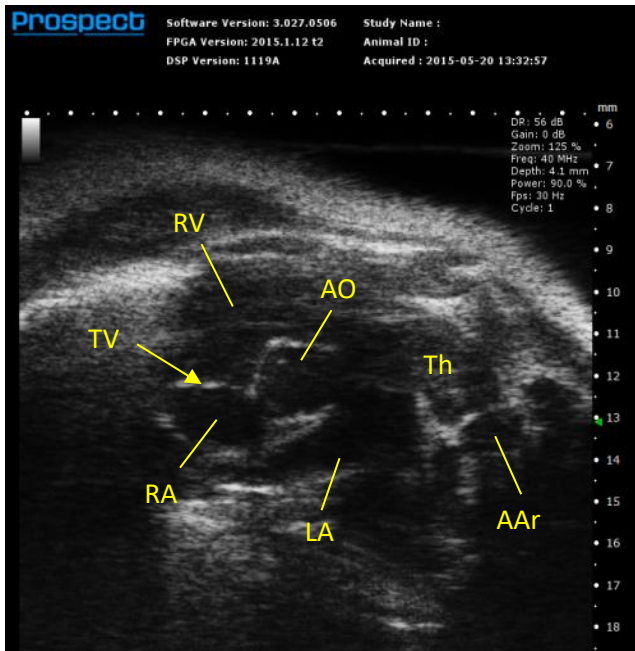
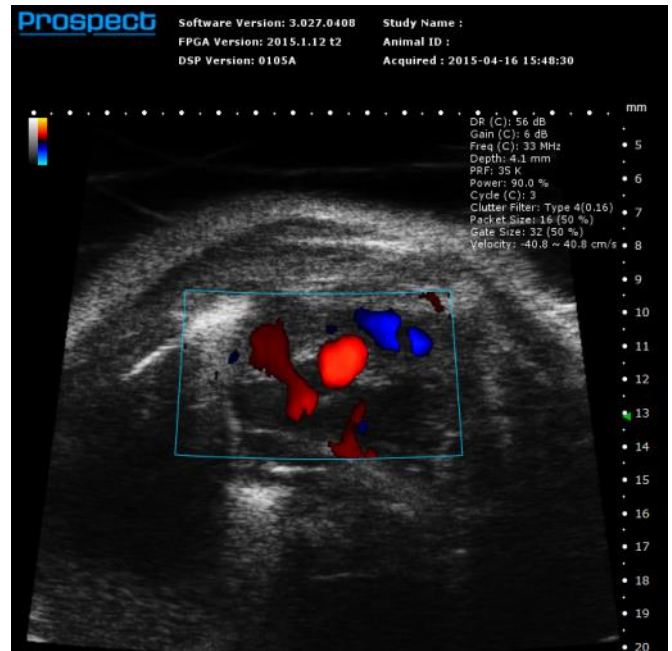


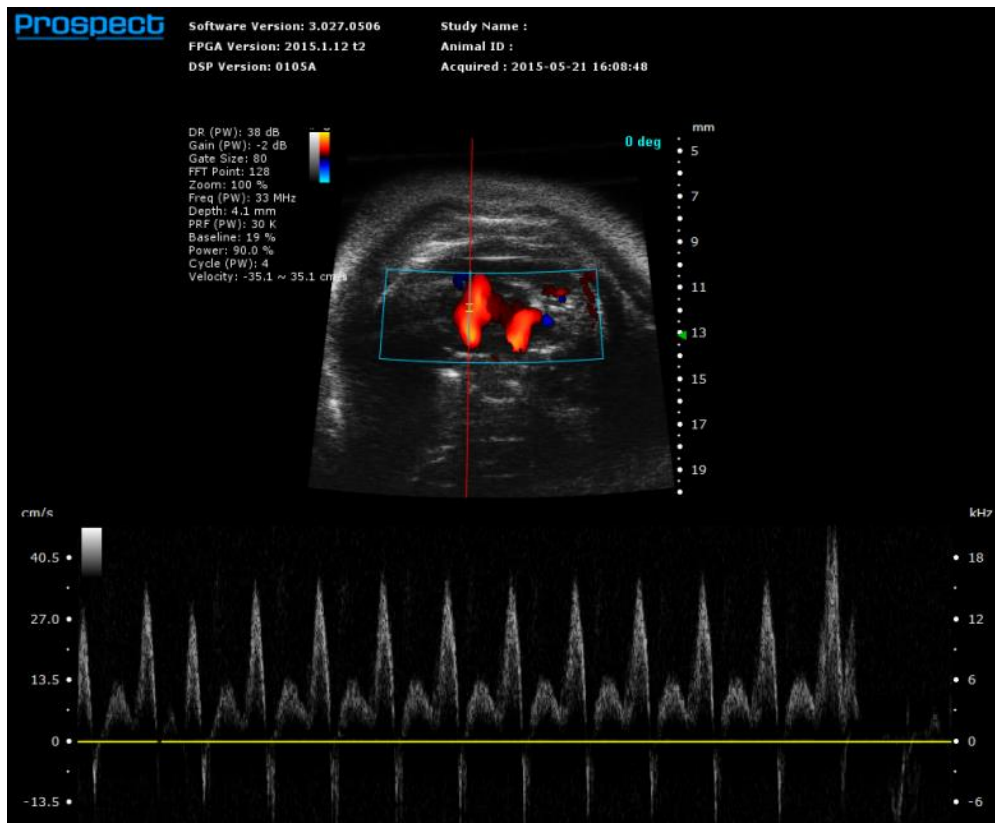
Fig. 6. Configuration of operation showing how to image the tricuspid valve (TV) in the right parasternal transverse section. (A) Long hinge position from the anterior view. (B) Short hinge position from the inferior view. (C) Transducer position.



(A)

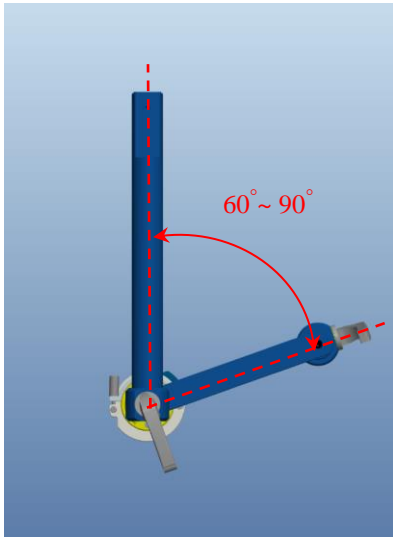


(B)

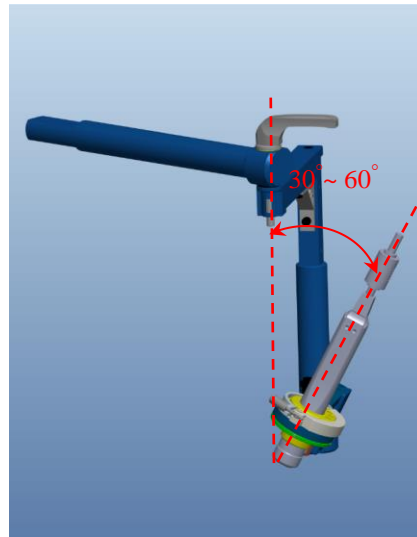


(C)

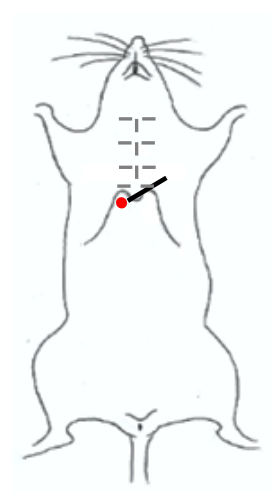
Fig. 7. TV imaging of the mouse in the right parasternal transverse section: (A) B-mode image, (B) color Doppler-mode image, and (C) PW-mode image. LA, left atrium; RV, right ventricle; AAr, aortic arch; AO, aortic orifice.



(A)

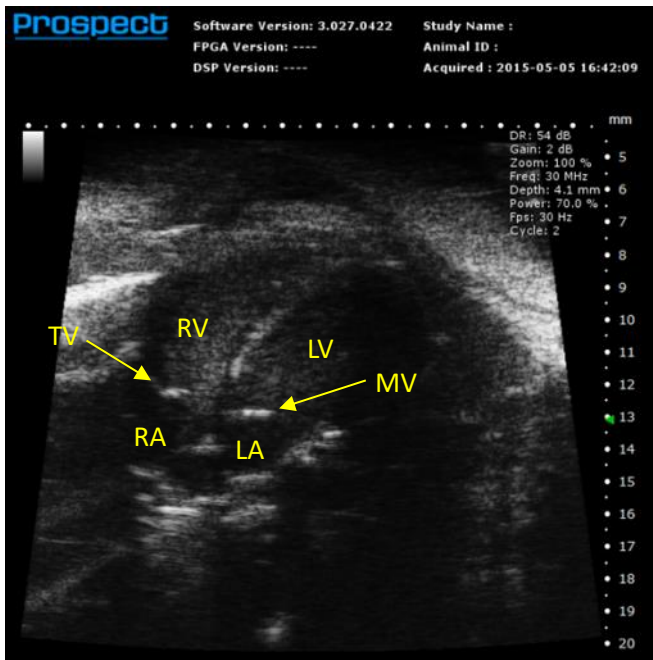


(B)

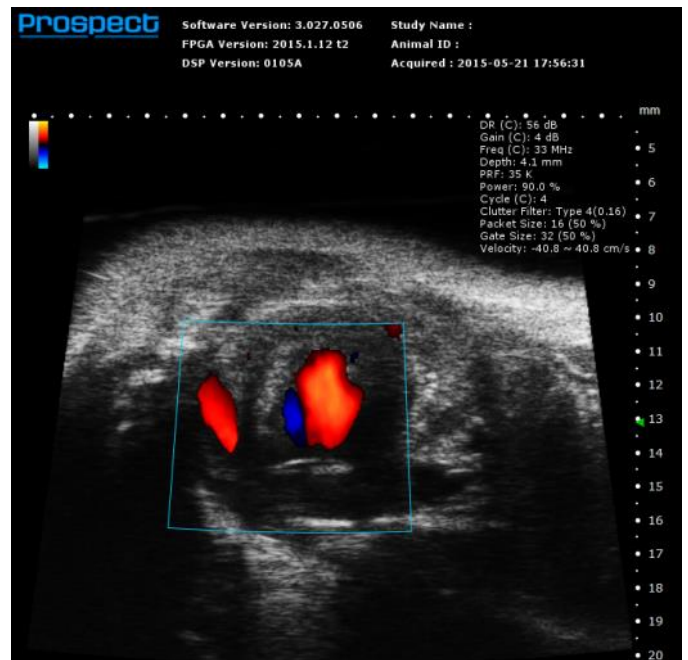


(C)

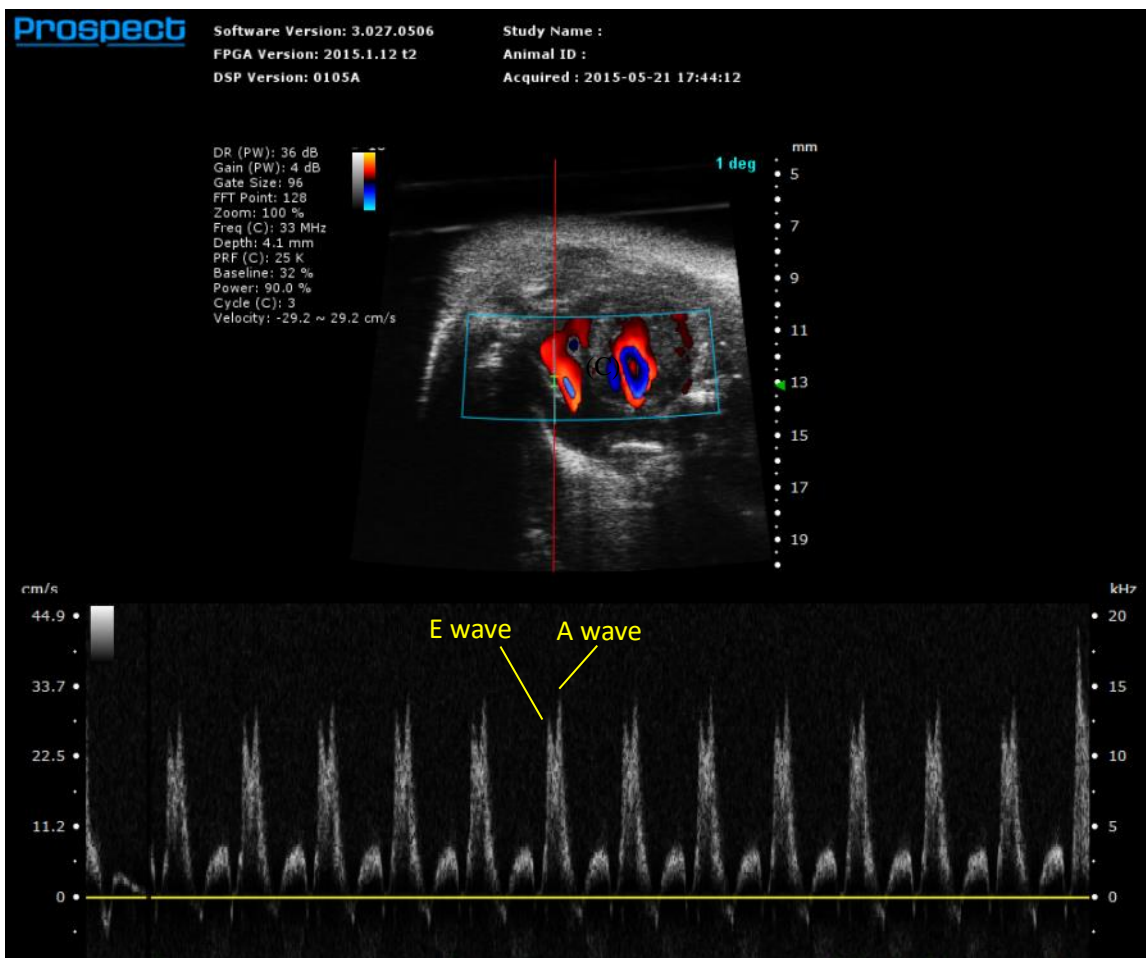
Fig. 8. Configuration of operation showing how to image the TV or mitral valve (MV) in the apical four-chamber view. (A) Long hinge position from the anterior view. (B) Short hinge position from the inferior view. (C) Transducer position.



(A)



(B)



(C)

Fig. 9. TV imaging of the mouse in the apical four-chamber view: (A) B-mode image, (B) color Doppler-mode image, and (C) PW-mode image.

D. Mitral Valve

The MV is easily observed by taking a longitudinal section in B-mode imaging from the right parasternal window or in the apical four-chamber view. To obtain an image of the MV from the right parasternal window, the long hinge of platform is first displaced clockwise by $0^{\circ}\sim 10^{\circ}$ from the anterior view, and then the short hinge of platform should be tilted counterclockwise by $60^{\circ}\sim 70^{\circ}$ from the inferior view. Finally, the transducer is orientated parallel to the central axis of the mouse's body and aimed at the lower one-third of its chest. The transducer's central axis is then aimed in the posterior direction (Fig. 10). This procedure will reveal the mitral orifice and MV, as well as the aortic orifice (AO) and ascending aorta (AAo), as shown in top half of Fig. 11. Furthermore, the M-mode image can be used to trace the valve movement in order to observe any defects therein. In particular, double peaks are present in the M-mode image at the anterior leaflet of the MV during the diastolic opening period (Fig. 11). The MV image can also be displayed in the apical four-chamber view, which is operated using the same method as for the TV section (Fig. 8). Similarly, the mitral Doppler flow spectrum is easily recorded by using PW-mode imaging, and it shows a larger E wave and a smaller A wave, with a slight decrease in the amplitude of the waveform during inspiration (Fig. 12).

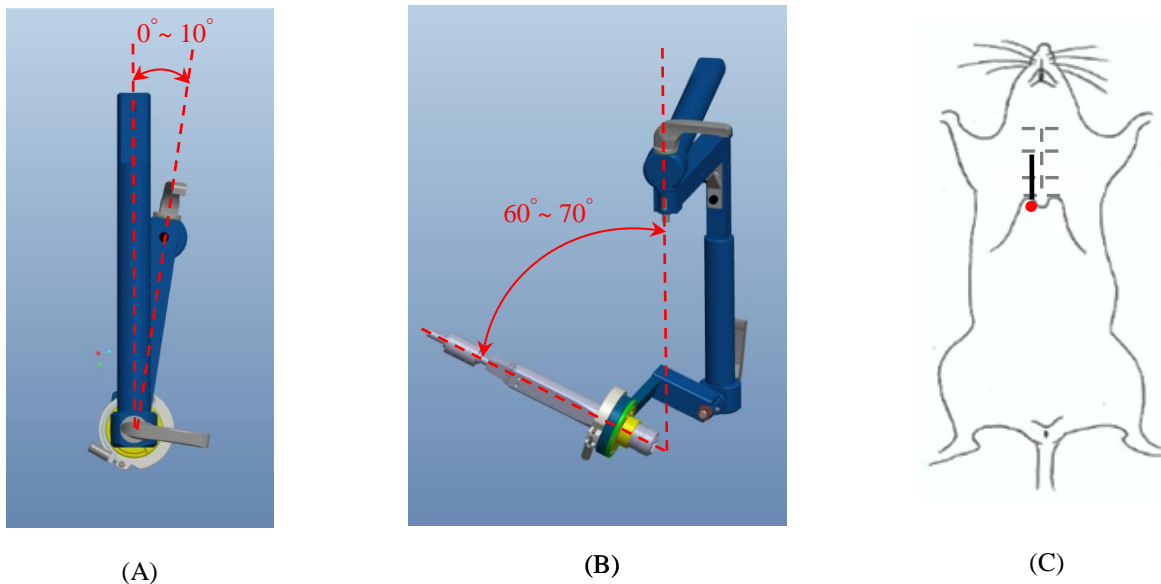


Fig. 10. Configuration of operation showing how to image the MV in the right parasternal longitudinal section. (A) Long hinge position from the anterior view. (B) Short hinge position from the inferior view. (C) Transducer position.

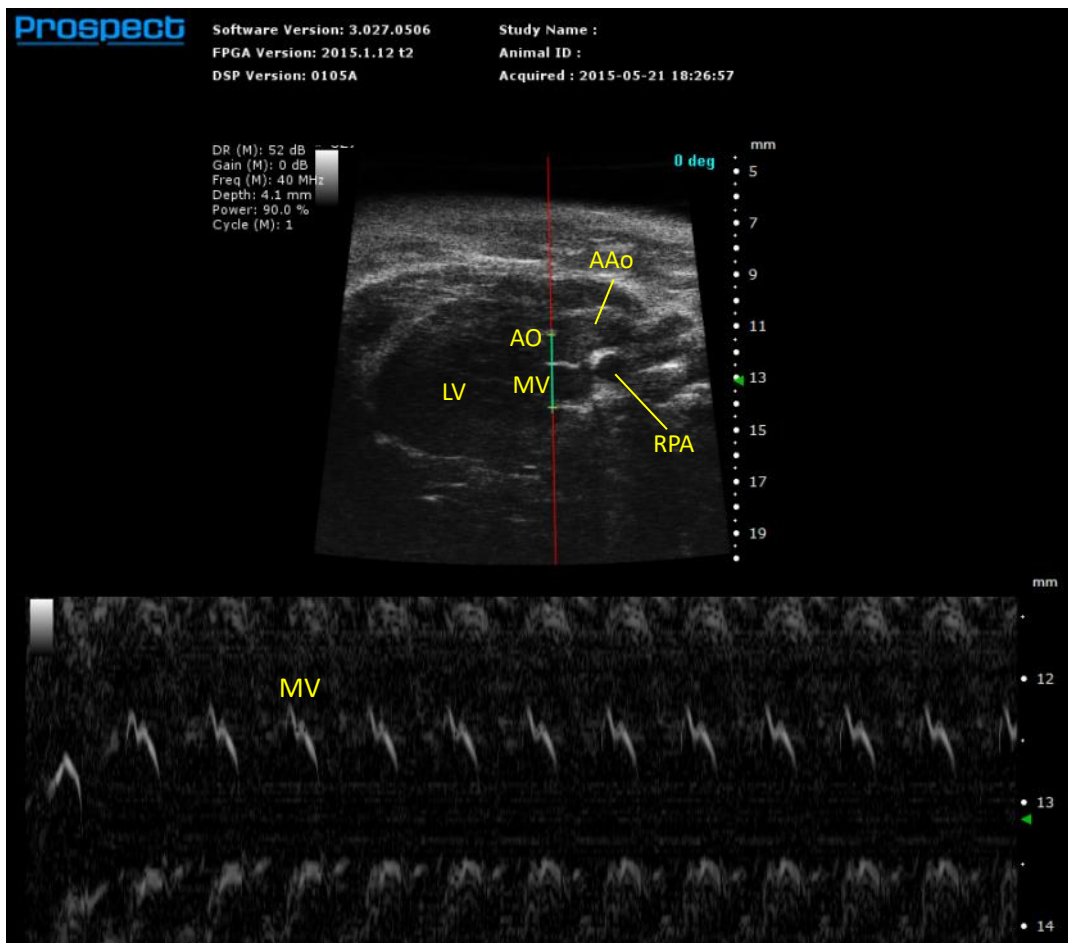
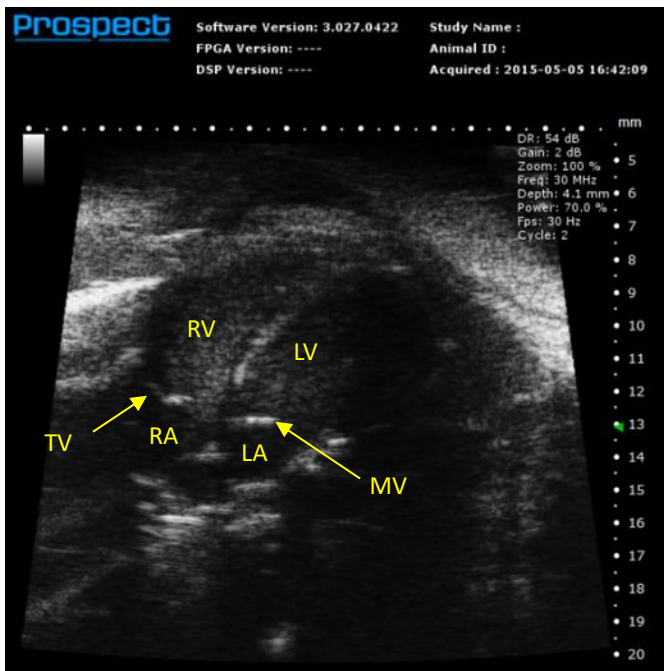
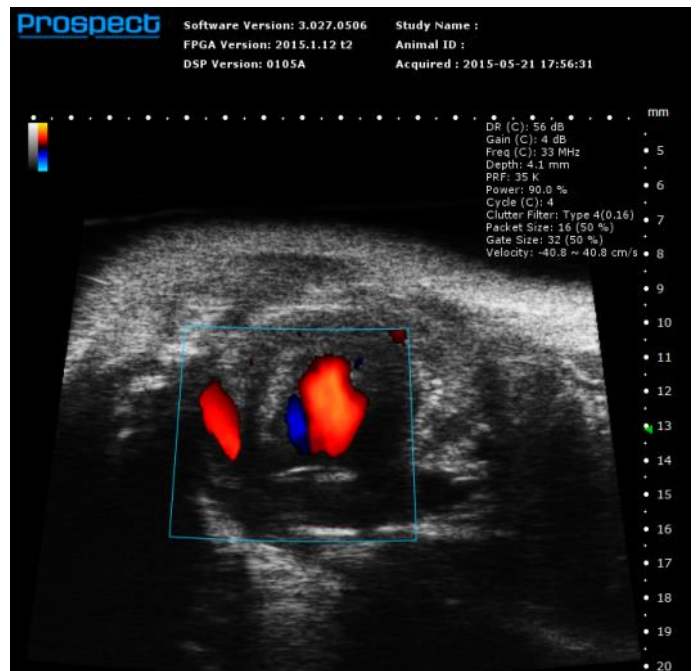


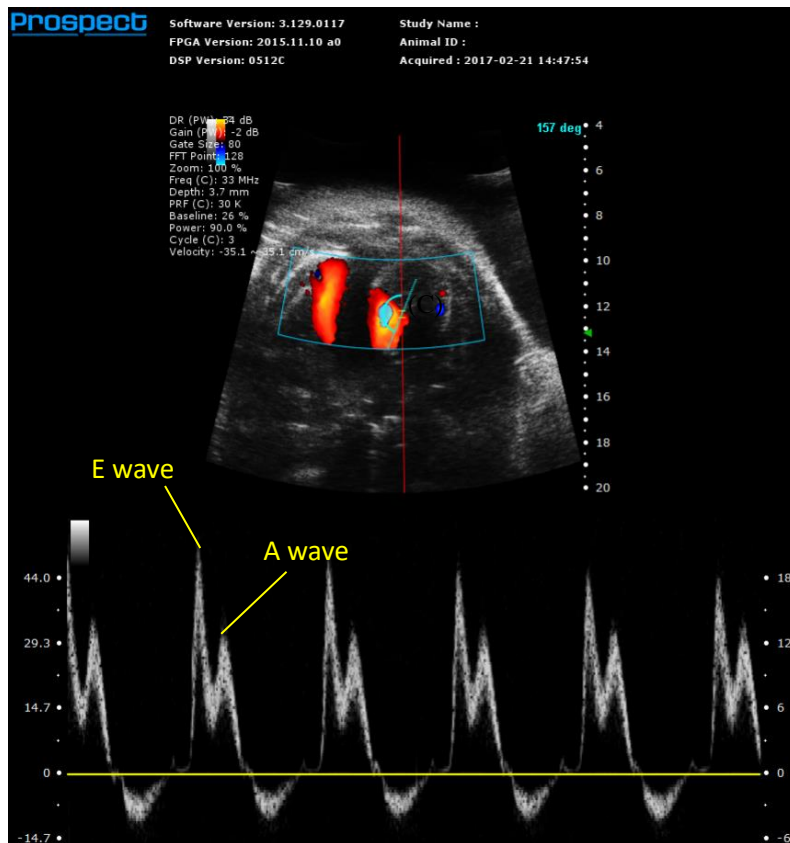
Fig. 11. MV imaging of the mouse in the right parasternal longitudinal section in M mode.



(A)



(B)



(C)

Fig. 12. Mitral valve imaging of the mouse in the apical four-chamber view: (A) B-mode image, (B) color Doppler-mode image, and (C) PW-mode image.

E. Parasternal Long-Axis View

The parasternal long-axis view (LA view) is usually evaluated initially because it can be used to assess the overall LV size and function. This is achieved by positioning the long hinge of platform clockwise by $60^{\circ}\sim 90^{\circ}$ from the anterior view, and the short hinge of platform must then be inclined clockwise (or counterclockwise) from the right side view by about 10° . The transducer should be orientated at the lower one-third of the chest, parallel to the central axis of mouse body, rotated $15^{\circ}\sim 30^{\circ}$ counterclockwise, and placed close to the surface (Fig. 13). It is necessary to visualize both the LVIT and LVOT in the same view. Thus, this view depicts the mid-portion and base of the LV, both leaflets of the MV, the aortic valve, and the aortic root [Fig. 14(A)]. Motion of the LV wall along the sampling line can be recorded and analyzed in M-mode imaging [Fig. 14(B)]. In addition, we provide the physical parameter measurements for cardiac applications. There are many cardiac indices available such as fractional shortening (FS), ejection fraction (EF), stroke volume (SV), cardiac output (CO) and so on. The operational steps of these cardiac indices measurements please refer to the Appendix A.

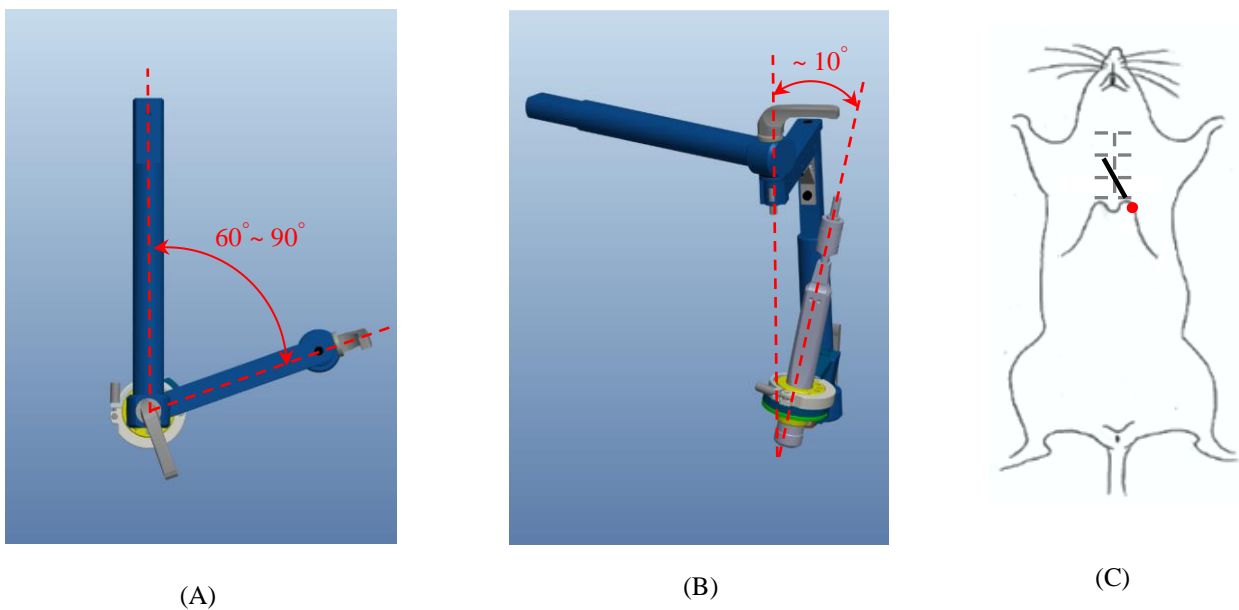
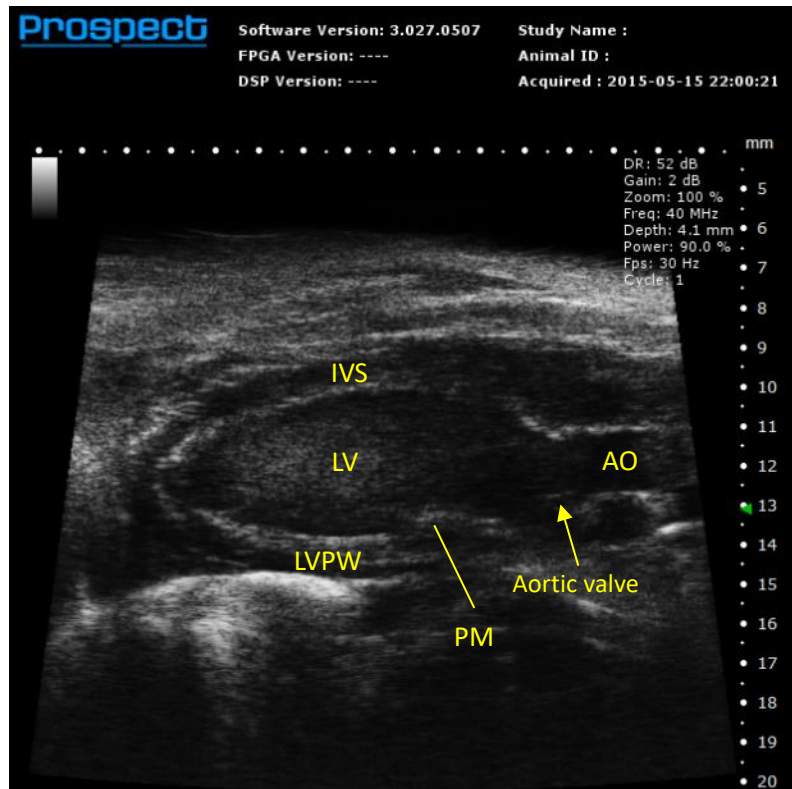
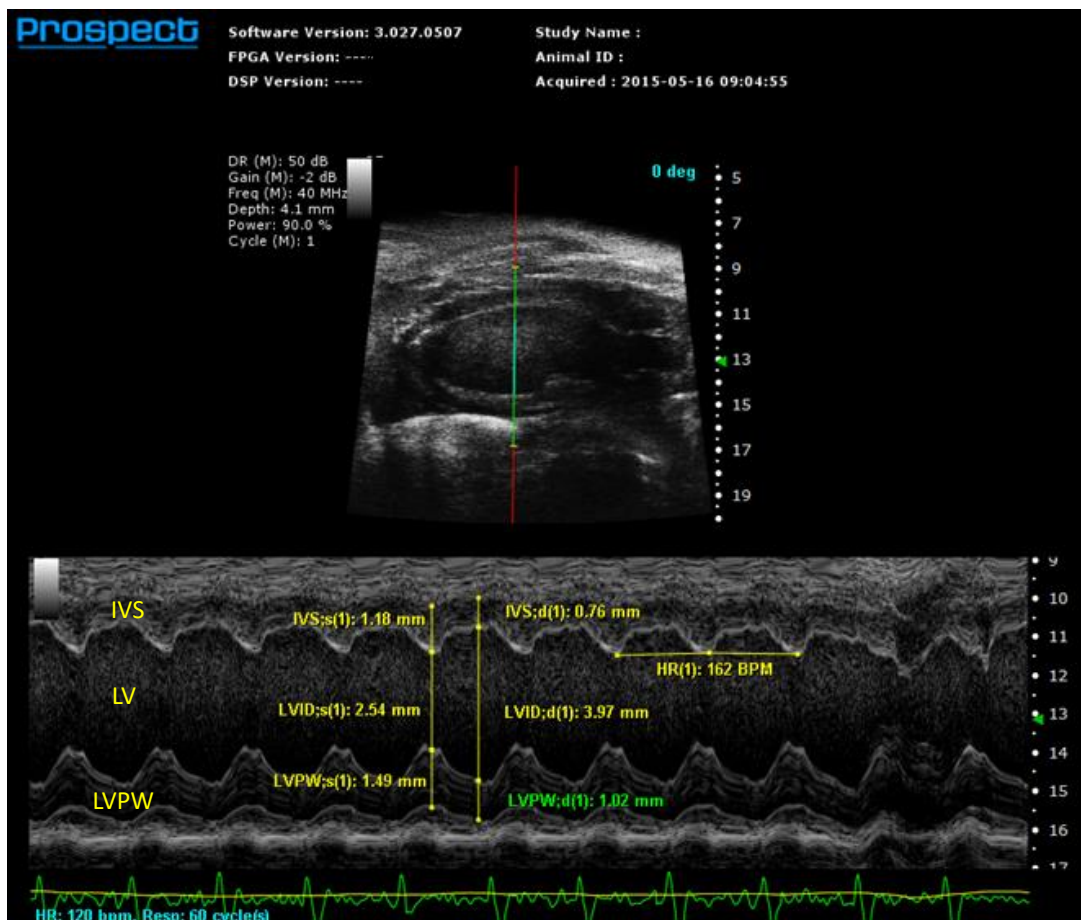


Fig. 13. Configuration of operation showing how to image the parasternal long-axis view (LA view) in the left parasternal longitudinal section. (A) Long hinge position from the anterior view. (B) Short hinge position from the inferior view. (C) Transducer position.



(A)



(B)

Fig. 14. LA-view imaging of the mouse: (A) B-mode image, (B) M-mode image showing the dimensional changes in the end-diastolic and end-systolic periods with the M-mode cursor line through its largest dimension. LVPW, left ventricular posterior wall; PM, papillary muscle.

F. The Parasternal Short-Axis View

The parasternal short-axis view (SA view) is most commonly used in M-mode imaging to estimate the LV structure and systolic function. In order to obtain an anatomically correct SA view, an LA view is usually imaged first. The SA view is obtained by rotating the transducer through 90° clockwise from the long-axis view (see Fig. 15). The transducer is then tilted slightly to the apex in order to visualize the papillary muscles (PMs). To ensure the reliability and repeatability of all measurements, the SA view at the PM level is required as a criterion for subsequent measurements made in the M-mode image. In other words, the LV is sectioned across the middle of the PMs and visualized as a completely round structure [Fig. 16(A)]. Similar to the LA view, motion of the LV wall along the sampling line can also be recorded and analyzed in the M-mode image [Fig. 16(B)]. Besides, the cardiac indices provided in the SA view are the same as in the LA view. Please refer to the Appendix A for more information.

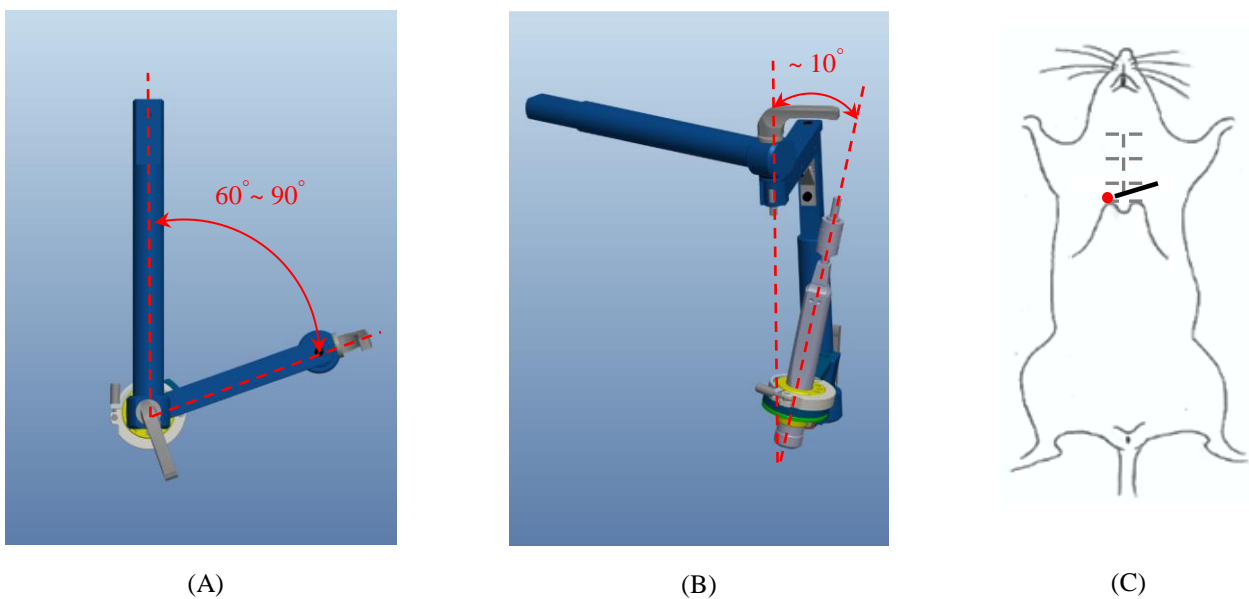
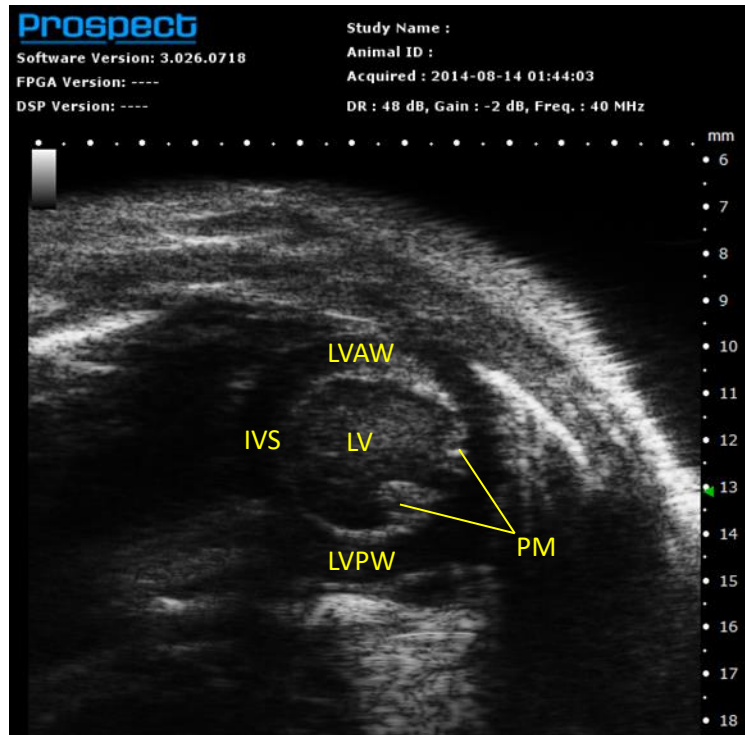
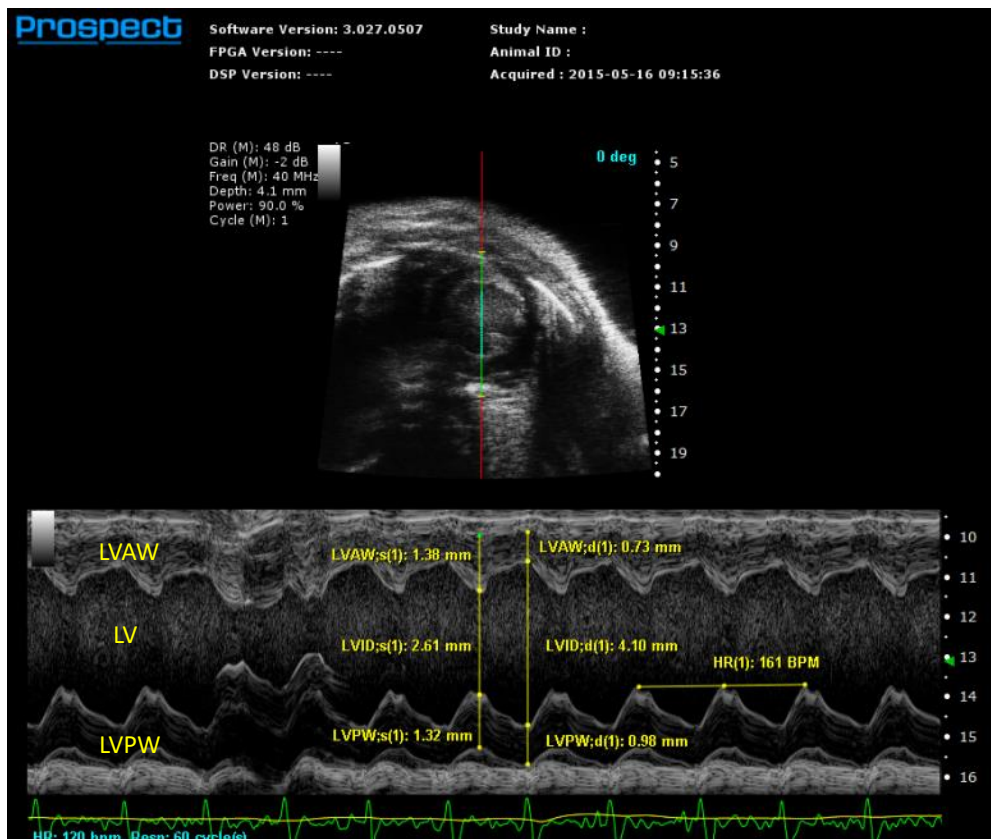


Fig. 15. Configuration of operation showing how to image the parasternal short-axis view (SA view) in the left parasternal transverse section. (A) Long hinge position from the anterior view. (B) Short hinge position from the inferior view. (C) Transducer position



(A)



(B)

Fig. 16. Parasternal short-axis view (SA view) imaging of the mouse: (A) B-mode image, (B) M-mode image with the M-mode cursor line through its largest dimension showing the dimensional changes in the end-diastolic and end-systolic periods. LVAW, left ventricular anterior wall.

G. Main Pulmonary Artery

The MPA is observed mainly in the left parasternal longitudinal section in B-mode imaging. Since the long hinge of platform should be moved counterclockwise by $30^{\circ}\sim 60^{\circ}$ from the anterior view, and then the short hinge of platform should be displaced clockwise by $10^{\circ}\sim 20^{\circ}$ from the left side view. Finally, the transducer is aimed at the middle one-third of the chest, almost parallel to the central axis of the mouse, and moved close to the surface (Fig. 17). The operational position of the platform for MPA also can be oriented at mirror symmetry position corresponded to the position described previously (long hinge: clockwise $30^{\circ}\sim 60^{\circ}$ and short hinge: counterclockwise $10^{\circ}\sim 20^{\circ}$). The MPA can be then located between the LA and aortic arch (AAr), and visualized [Fig. 18(A)]. Its blood velocity can be estimated by using PW-mode imaging with a small Doppler angle [Fig. 18(B) and (C)].

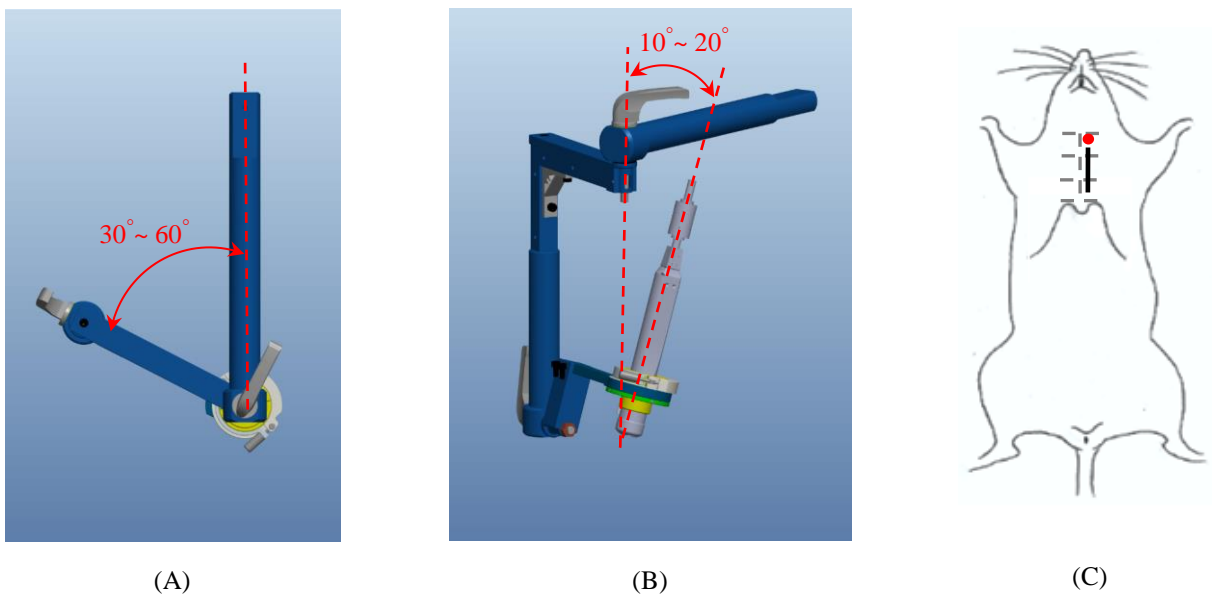
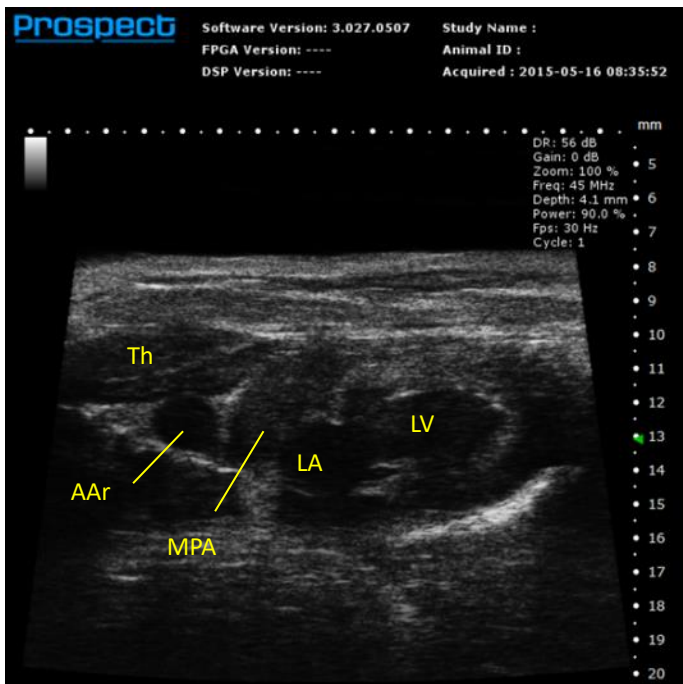
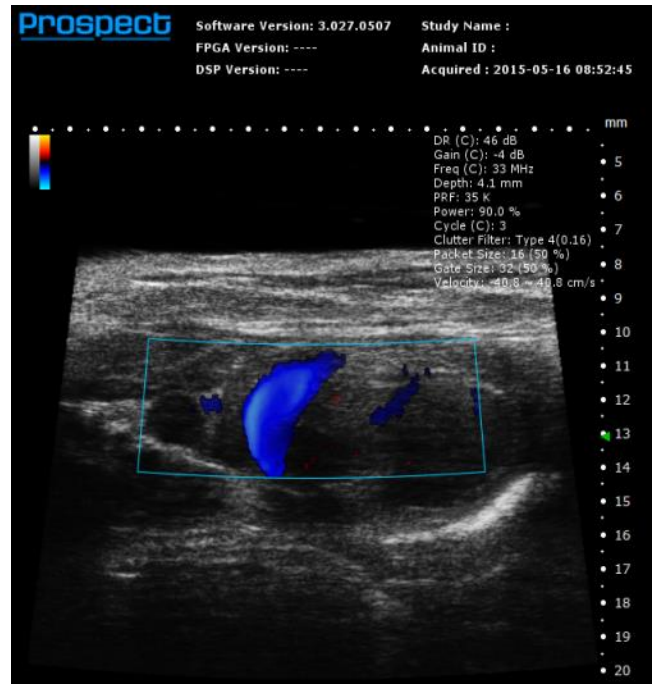


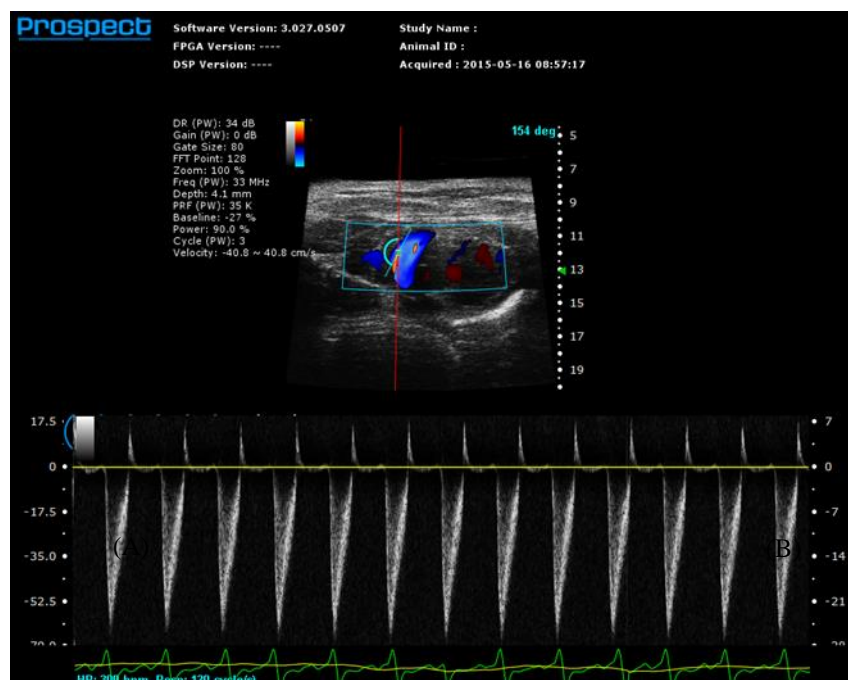
Fig. 17. Configuration of operation showing how to image the main pulmonary artery (MPA) in a left parasternal longitudinal section. (A) Long hinge position from the anterior view. (B) Short hinge position from the inferior view. (C) Transducer position.



(A)



(B)



(C)

Fig. 18. MPA imaging of the mouse: (A) B-mode image, (B) color Doppler-mode image, and (C) PW-mode image with the Doppler sampling volume at its lumen showing its Doppler flow spectrum and blood velocity.

H. Right Ventricular Outflow Tract

The right ventricular outflow tract (RVOT) can be visualized by imaging the left parasternal longitudinal section. The long hinge of platform should be moved counterclockwise by $0^{\circ}\sim 10^{\circ}$ from the anterior view, and the short hinge of platform should be displaced clockwise from the inferior view by about 40° from the inferior view. The transducer should be positioned at the middle one-third of the chest and aimed in the posterior direction (Fig. 19). The RVOT would then appear in the location where is closer to the transducer along with the LVOT, while the AAo, RA, and RV should be visualized further away from the transducer [Fig. 20(A)]. Because of their presence in the same beam direction, dimensional changes of the RVOT, AAo, and RA can be recorded simultaneously during the cardiac cycle by using M-mode imaging [Fig. 20(B)].

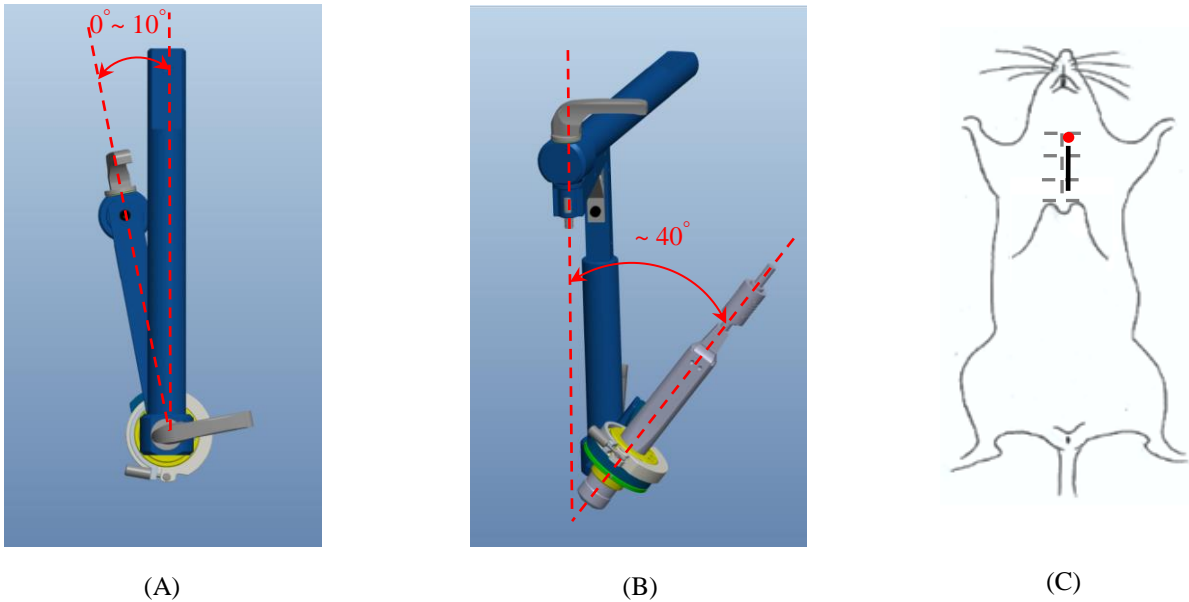
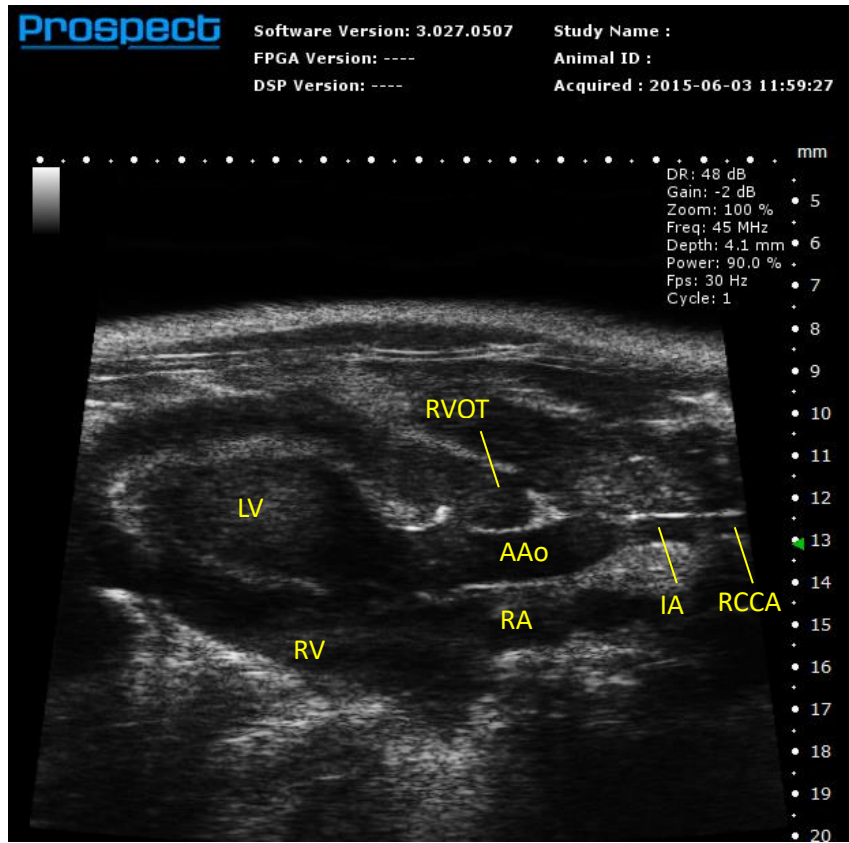
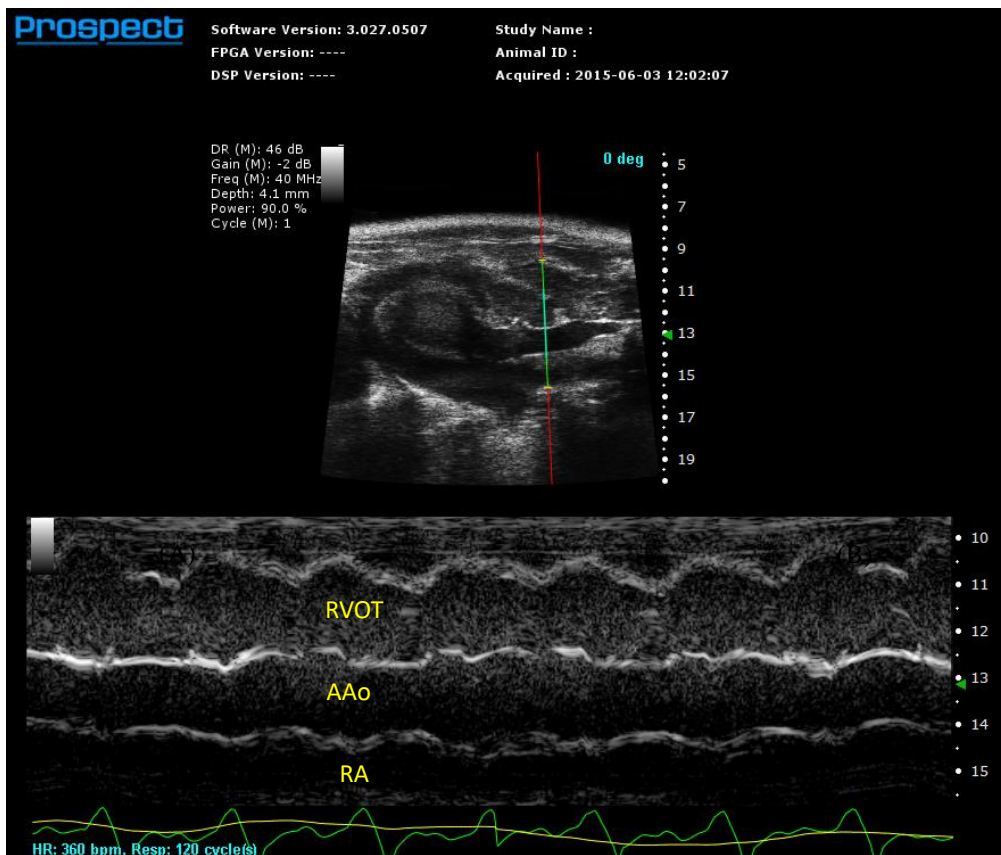


Fig. 19. Configuration of operation showing how to image the right ventricular outflow tract (RVOT) in a left parasternal longitudinal section. (A) Long hinge position from the anterior view. (B) Short hinge position from the inferior view. (C) Transducer position.



(A)



(B)

Fig. 20. RVOT imaging of the mouse:(A) B-mode image, (B) B-mode image with the M-mode cursor line over the RVOT, AAO, and RA, demonstrating the dimensional changes of the RVOT, AAO, and RA. IA, innominate artery; RCCA, right common carotid artery.

I. Aortic Orifice and Ascending Aorta

The LVOT starts at the AO, where the blood leaves the heart, and continues via the AAo. From the right parasternal window there are two approaches to image the AO and AAo. The first is the upper right parasternal approach. This is accomplished by positioning the long hinge of platform clockwise by $60^{\circ}\sim 90^{\circ}$ from the anterior view, and displacing the short hinge of platform counterclockwise by $0^{\circ}\sim 20^{\circ}$ from the right side view. The transducer should be oriented at the upper one-third of the chest, almost parallel to the central axis of mouse, and close to the surface (Fig. 21). In this view the AAo appears along its longitudinal axis in the B-mode image and its blood velocity can be estimated by PW-mode imaging (Fig. 22). The second approach is the lower right parasternal approach, wherein the long hinge of platform tilted clockwise by $0^{\circ}\sim 30^{\circ}$ from the anterior view, and the short hinge of platform moved counterclockwise by about 40° from the inferior view. The transducer is positioned at the lower one-third of the chest, parallel to the central axis of mouse's body, and aimed at the posterior section of the mouse (Fig. 23). In this view the AO and AAo are more clearly visible in the B-mode image. The M-mode image demonstrates the movement of the aortic cusps and the changing diameter of the AAo during the cardiac cycle (Figs. 24 and 25).

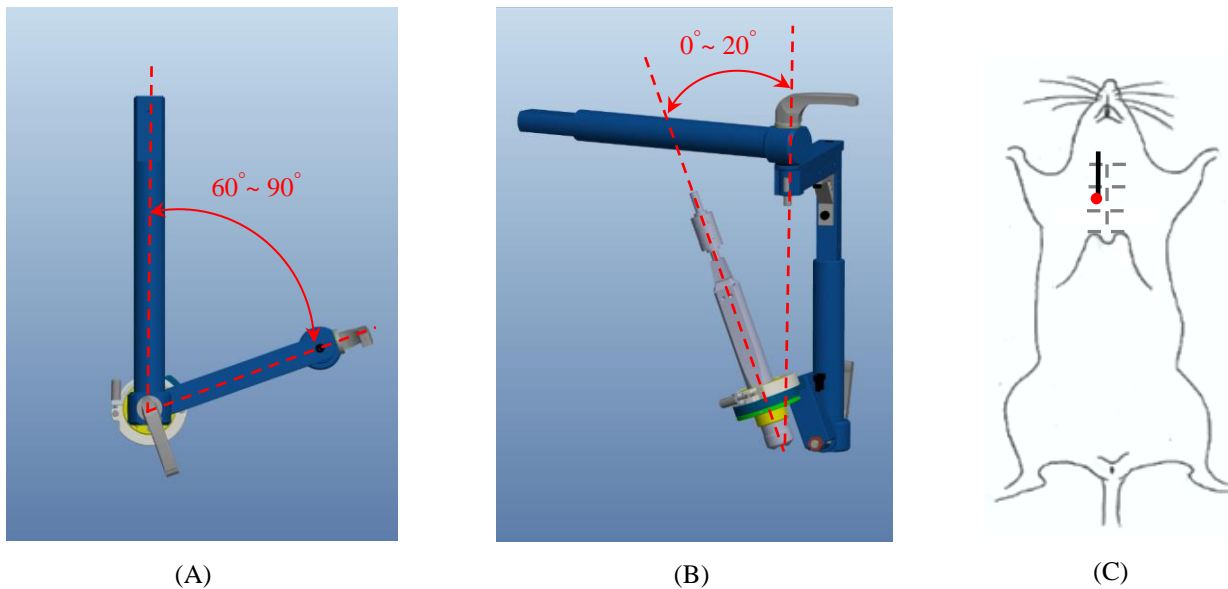
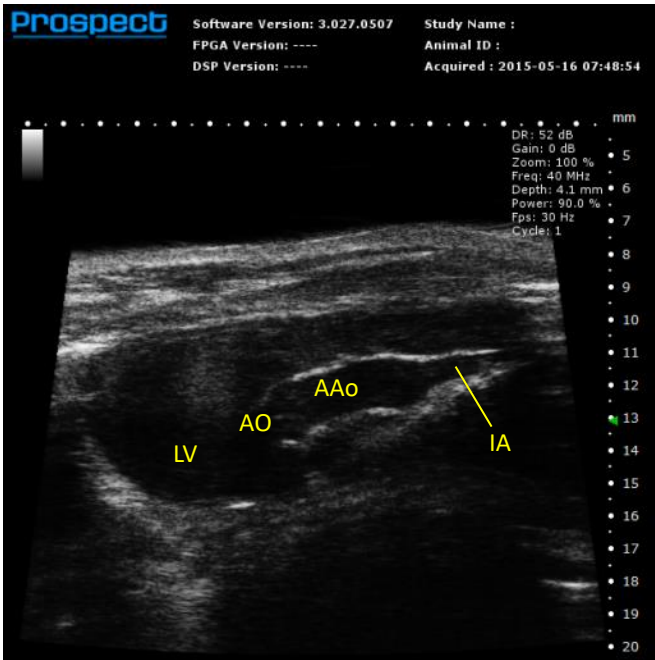


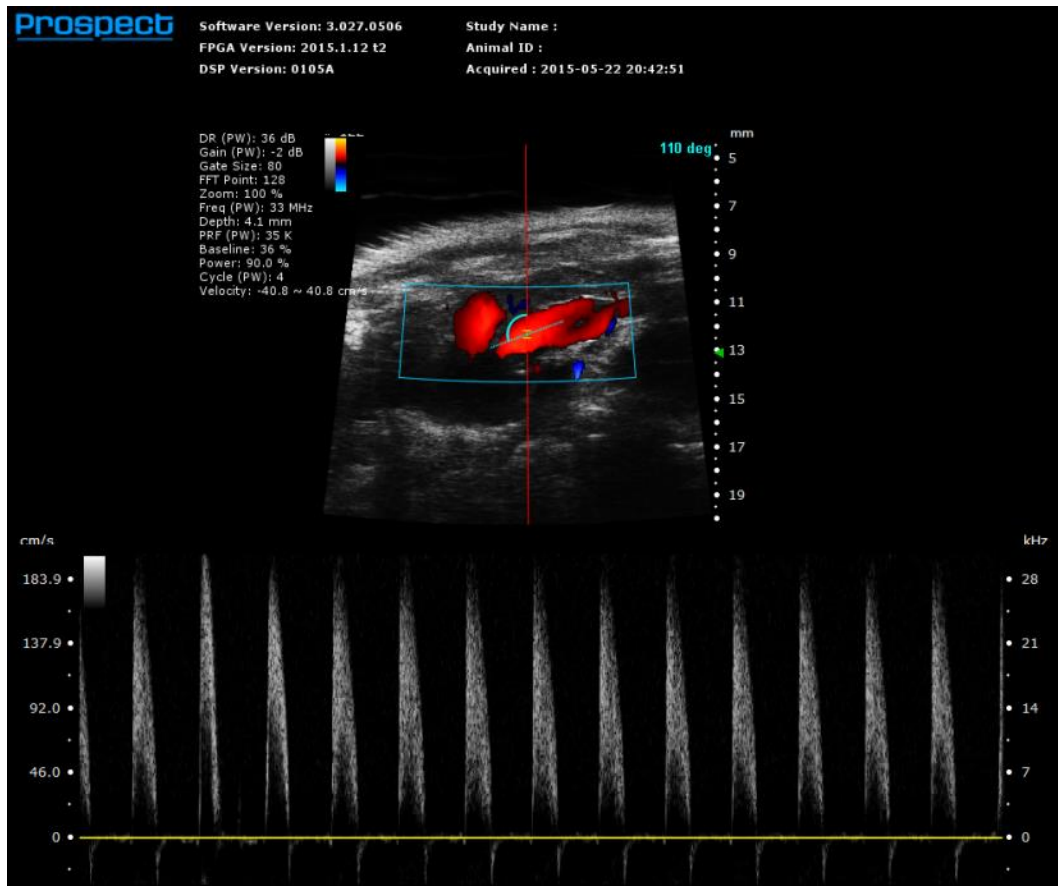
Fig. 21. Configuration of operation showing how to image the AO and AAo in the right parasternal longitudinal section. (A) Long hinge position from the anterior view. (B) Short hinge position from the inferior view. (C) Transducer position.



(A)



(B)



(C)

Fig. 22. AO and AAO imaging of the mouse: (A) B-mode image, (B) color Doppler-mode image, and (C) PW-mode image of the AAO showing its blood velocity.

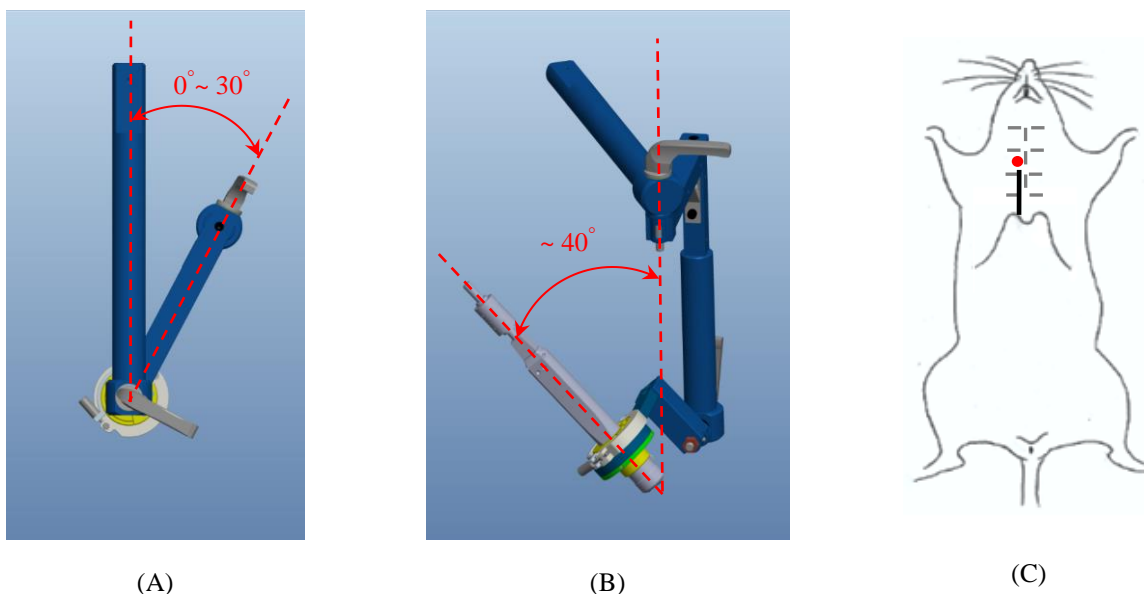


Fig. 23. Configuration of operation showing how to image the AO and AAo in the right parasternal longitudinal section. (A) Long hinge position from the anterior view. (B) Short hinge position from the inferior view. (C) Transducer position.

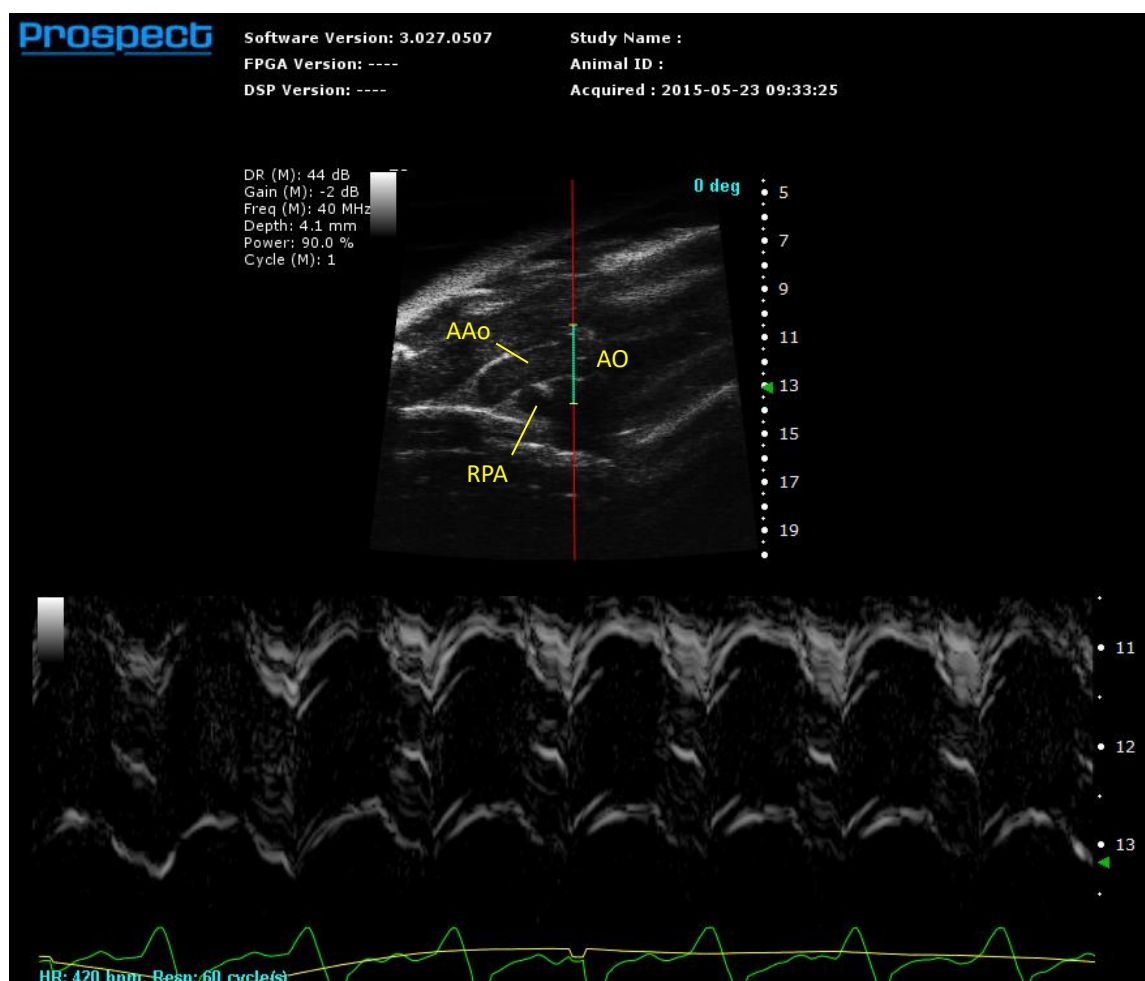


Fig. 24. AO and AAo imaging of the mouse: M-mode recording at the level of AO showing the movement of the aortic cusps with the M-mode cursor line cross the aortic cusps.

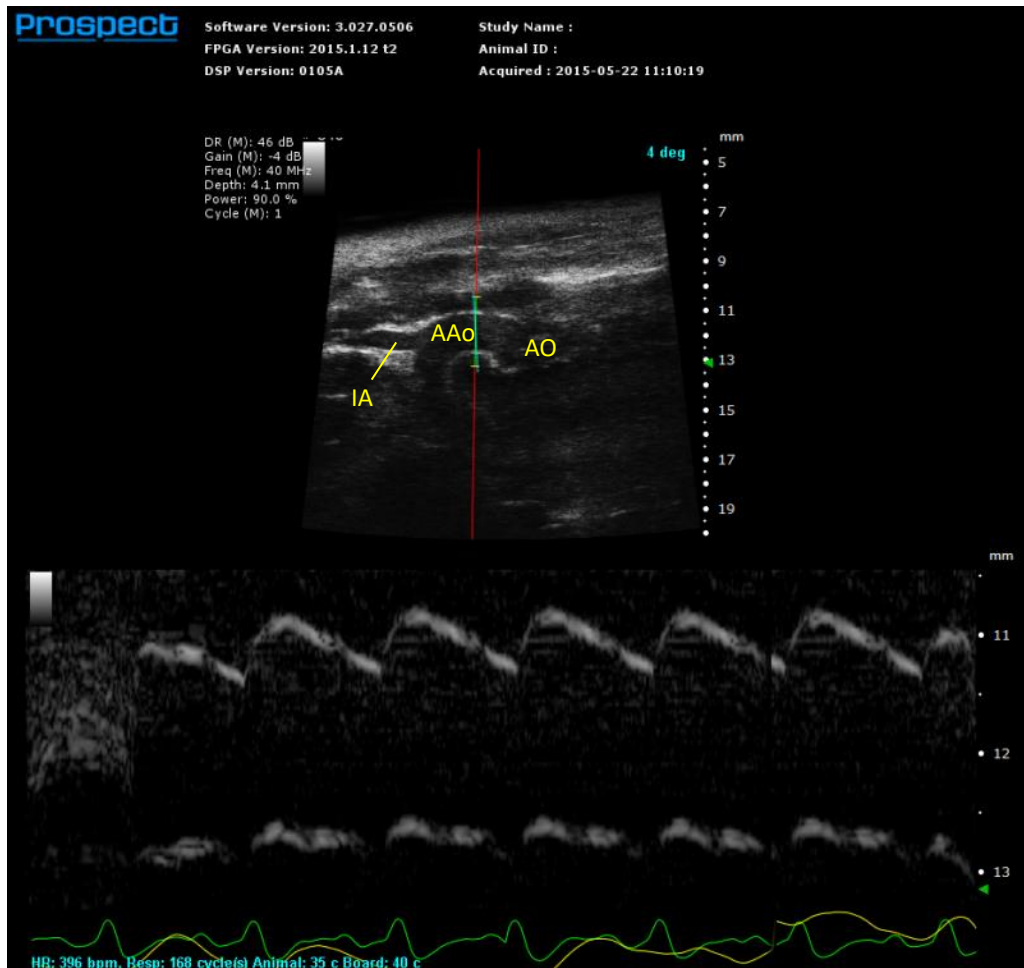


Fig. 25. AO and AAO imaging of the mouse: M-mode image of the AAO showing the dimension changes in the end-diastolic and end-systolic periods with the M-mode cursor line cross the AAO.

J. Left Coronary Artery

The LCA can be imaged in a left parasternal transverse section by positioning the transducer at the middle one-third of the chest, perpendicular to the central axis of mouse body, rotated around 15° clockwise, and aimed toward the surface. The long hinge of platform should be displaced clockwise by $0^\circ\sim 10^\circ$ from the anterior view, and the short hinge of platform must be inclined counterclockwise from the inferior view by $60^\circ\sim 70^\circ$ (Fig. 26). The B-mode image displays the proximal part of the LCA [Fig. 27(A)]. In PW-mode imaging, the Doppler flow spectrum recorded from the proximal part of the LCA reveals a continuous and pulsatile flow pattern during the cardiac cycle, as shown in Fig. 27(B) and (C).

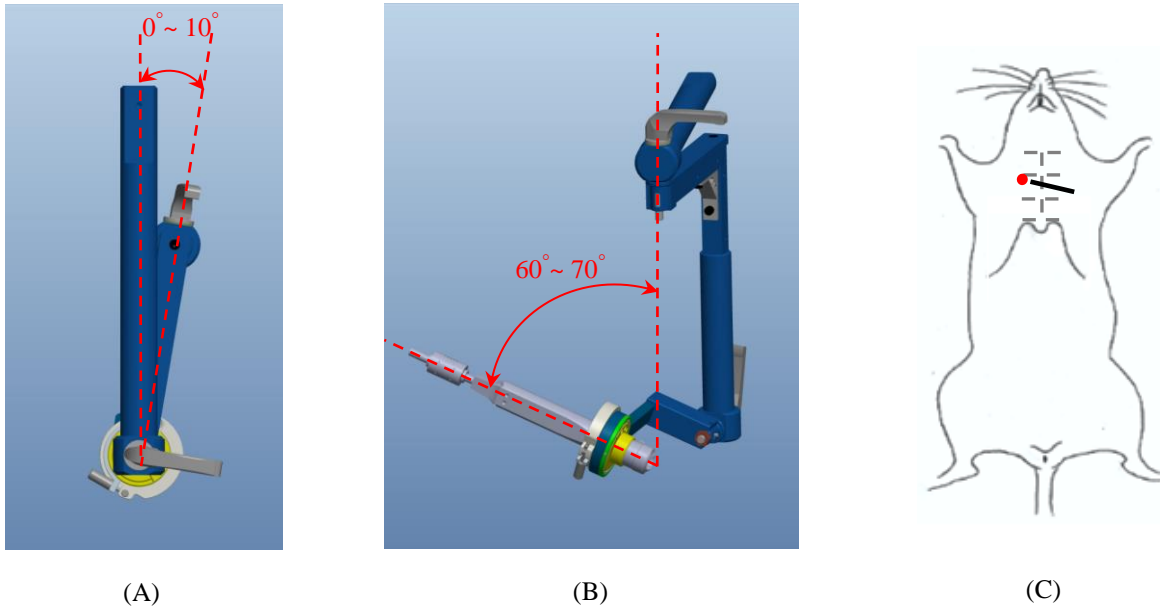
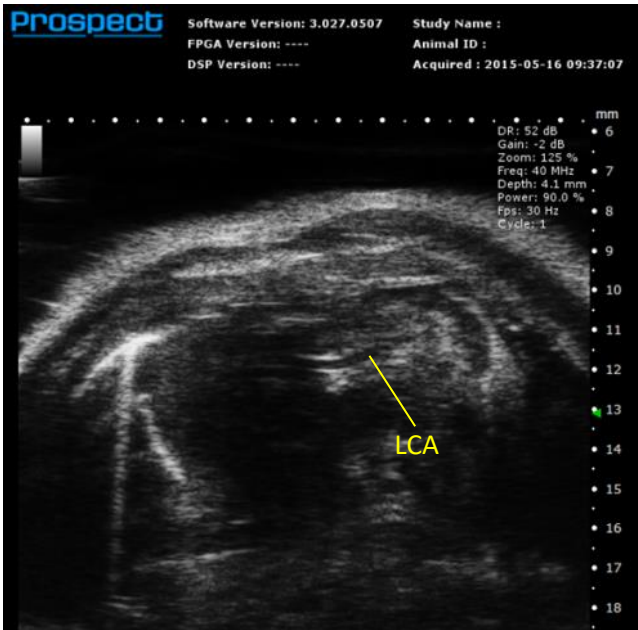
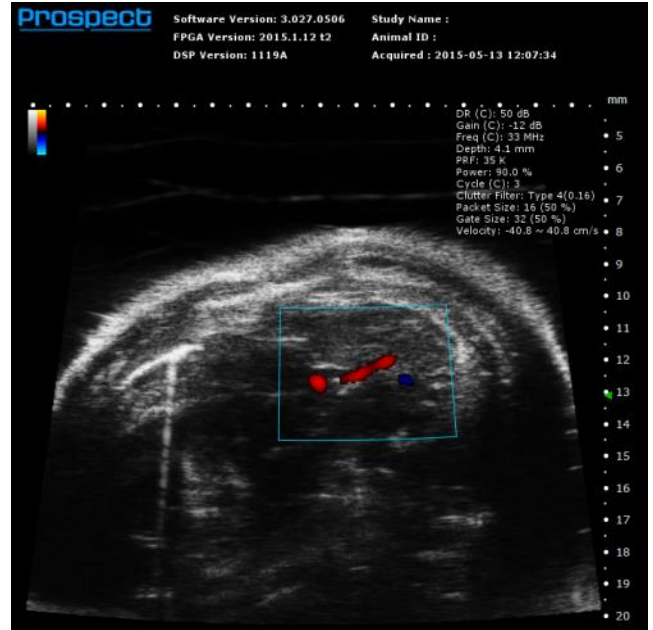


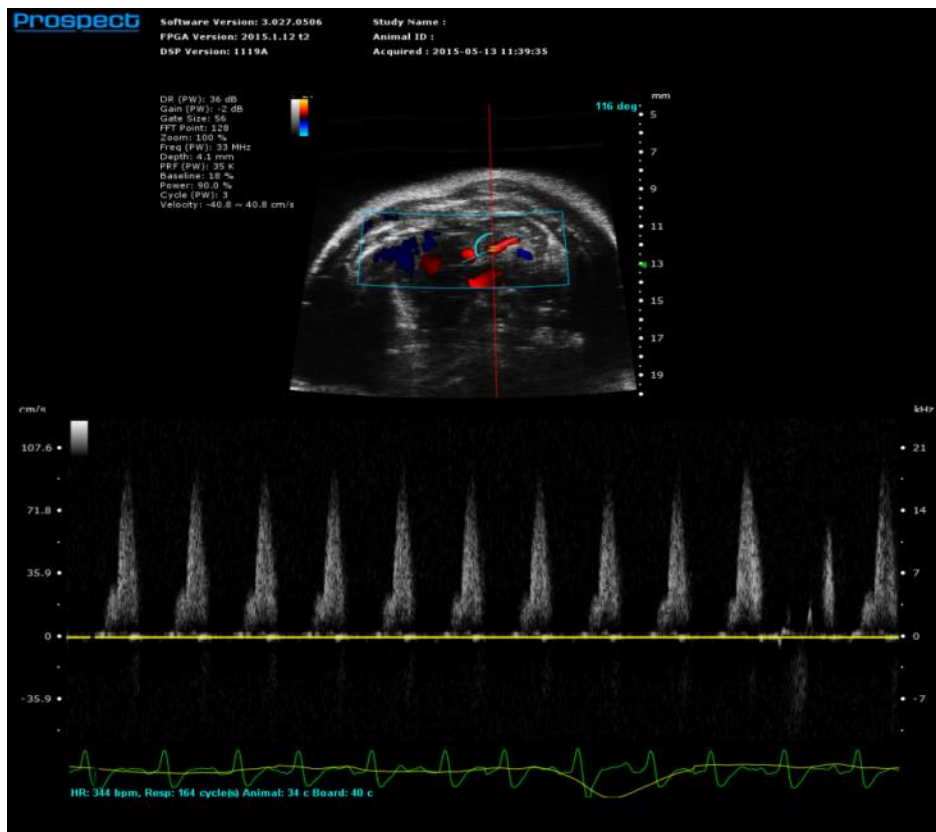
Fig. 26. Configuration of operation showing how to image the left coronary artery (LCA) in the left parasternal transverse section. (A) Long hinge position from the anterior view. (B) Short hinge position from the inferior view. (C) Transducer position.



(A)



(B)



(C)

Fig. 27. LCA imaging of the mouse: (A) B-mode image, (B) color Doppler-mode image, and (C) PW-mode image.

K. Aortic Arch

The entire AAr and its three branches, the innominate artery (IA), left common carotid artery (LCCA) and left subclavian artery (LSCA), are easily visualized only in a right parasternal longitudinal section with the long hinge of platform tilted clockwise by $0^{\circ}\sim 30^{\circ}$ from the anterior view, and with the short hinge of platform moved counterclockwise by $45^{\circ}\sim 60^{\circ}$ from the inferior view (Fig. 29). The transducer should be positioned at the middle one-third of the chest, parallel to the central axis of the mouse, and moved close to the surface (Fig. 28).

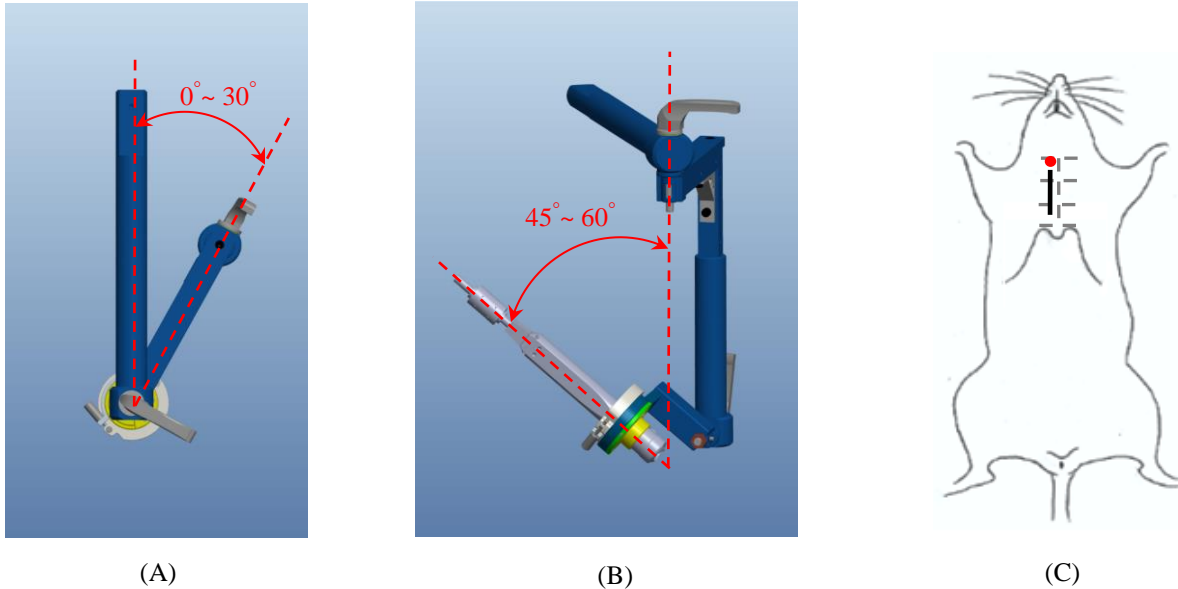


Fig. 28. Configuration of operation showing how to image the AAr in the right parasternal longitudinal section. (A) Long hinge position from the anterior view. (B) Short hinge position from the inferior view. (C) Transducer position.

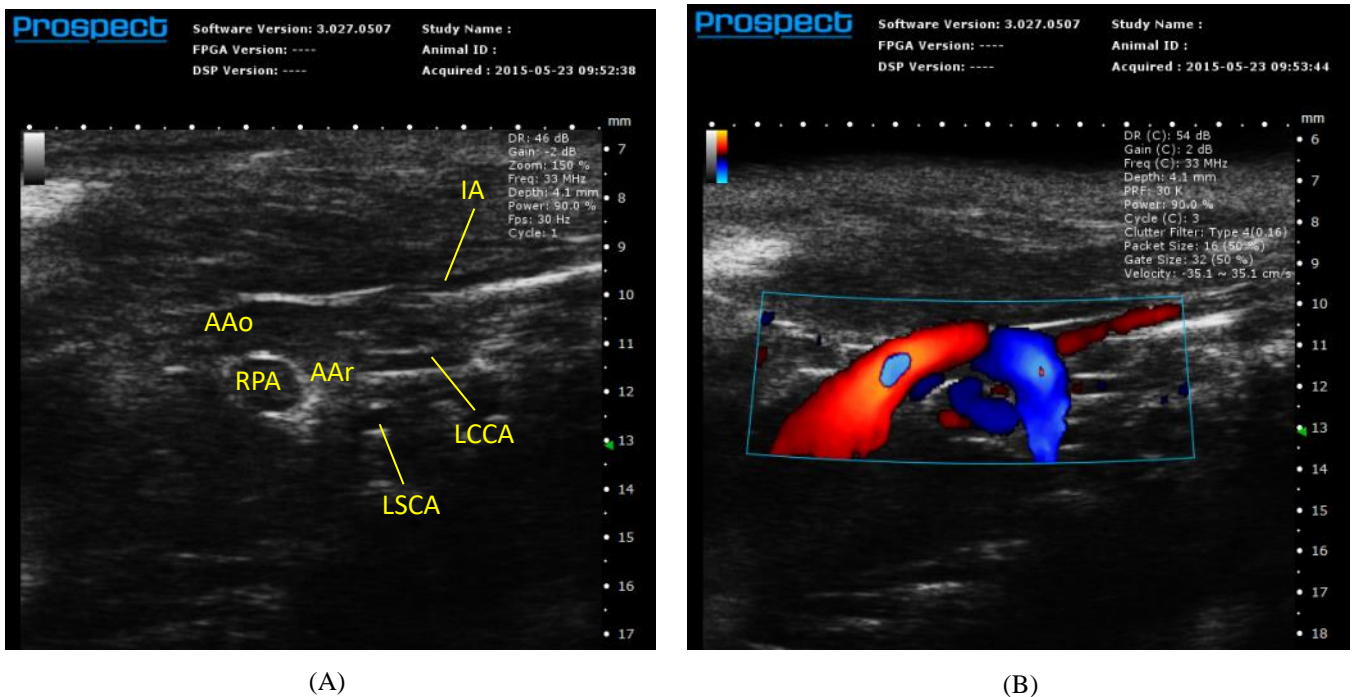


Fig. 29. AAr imaging of the mouse: (A) B-mode image of the entire AAr and the proximal parts of its three branches: IA, left common carotid artery (LCCA), and left subclavian artery (LSCA). (B) color Doppler-mode image.

L. Right Common Carotid Artery

The major branches of the mouse aorta are similar to those in humans. The right IA leaves the AAr and is divided into the right common carotid artery (RCCA) and the right subclavian artery. The IA and the downstream RCCA also can be visualized in the right parasternal longitudinal section. The long hinge of platform should be adjusted clockwise by $0^{\circ}\sim 10^{\circ}$ from the anterior view, and then the short hinge of platform should be tilted counterclockwise by about 60° from the inferior view. The transducer should be positioned at the middle one-third of chest, parallel to the central axis of the mouse, and close to the surface (Fig. 30). This view makes it possible to observe the RCCA clearly as well as the AAr and IA in the B-mode image (Fig. 31).

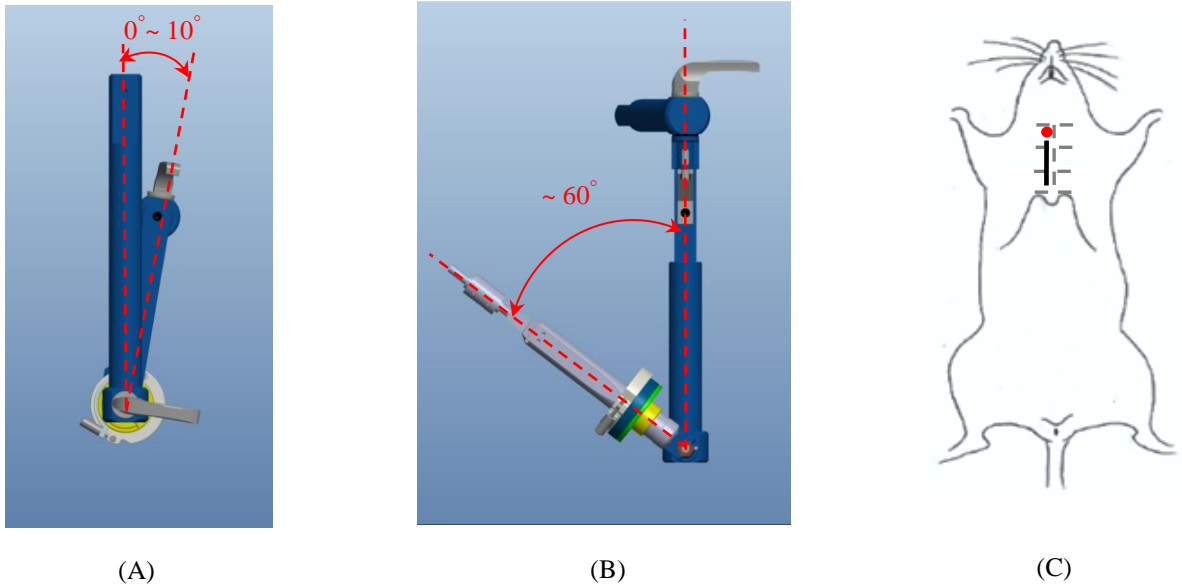
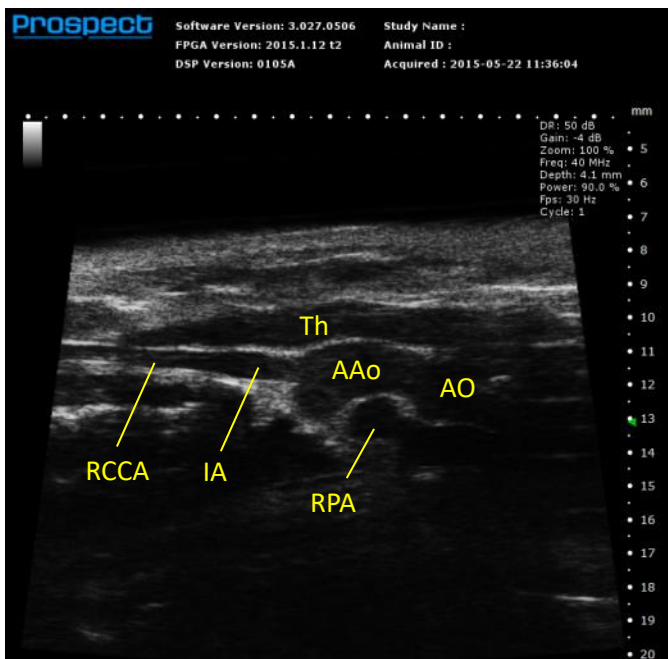


Fig. 30. Configuration of operation showing how to image the right common carotid artery (RCCA) in the right parasternal longitudinal section. (A) Long hinge position from the anterior view. (B) Short hinge position from the inferior view. (C) Transducer position.



(A)



(B)



(C)

Fig. 31. RCCA imaging of the mouse: (A) B-mode image showing the RCCA, AAo, and IA, (B) color Doppler-mode in distal RCCA and its branch is also displayed clearly, and (C) PW-mode image.

M. Left Common Carotid Artery

In the mouse, the LCCA leaves the AAr and the RCCA leave the right subclavical artery separated by approximately 1 mm, where they run parallel up the animal's neck. Therefore, the longitudinal section of the LCCA is shown in the B-mode image (Fig. 32) in the same position as the RCCA but moved leftward in parallel in the left parasternal longitudinal section (Fig. 33).

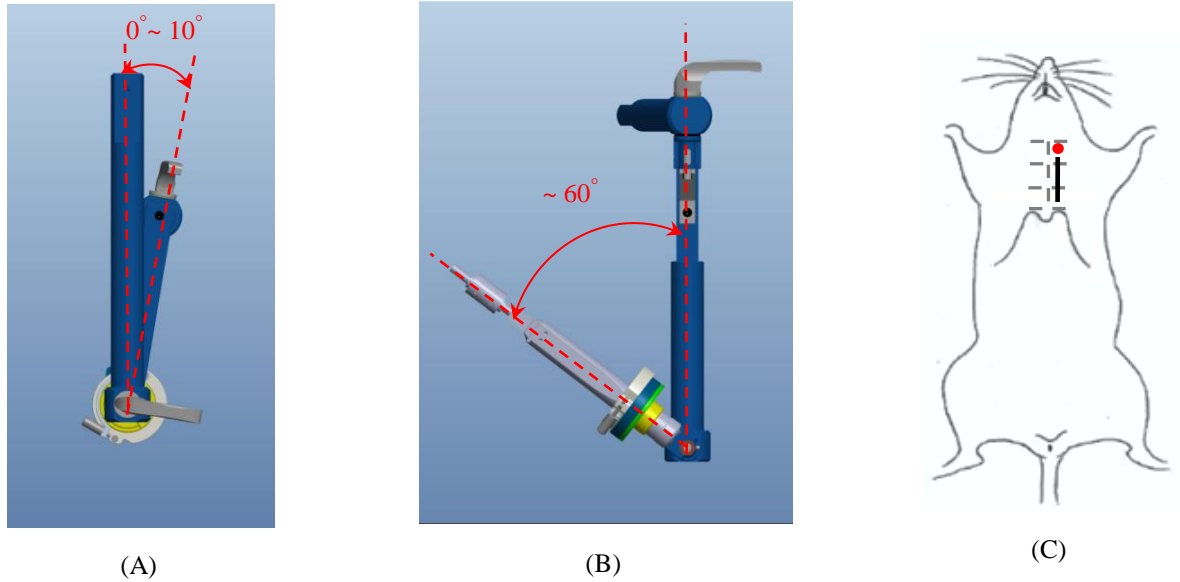
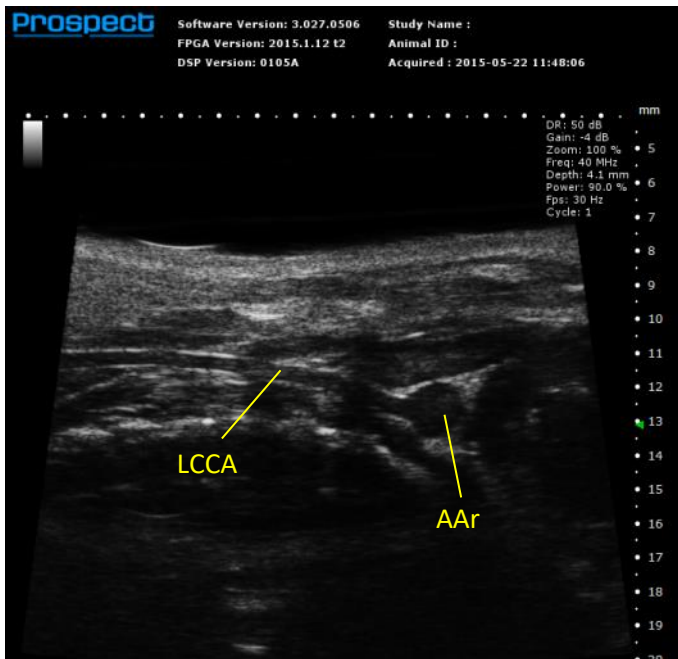
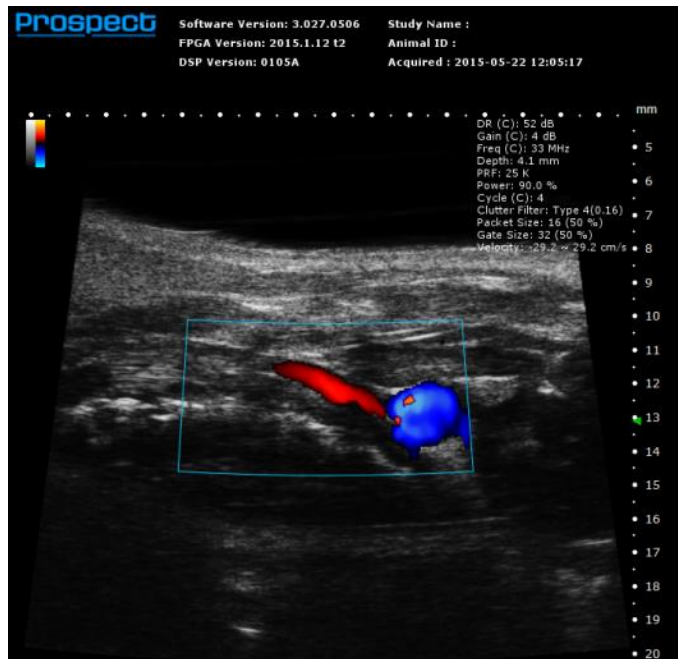


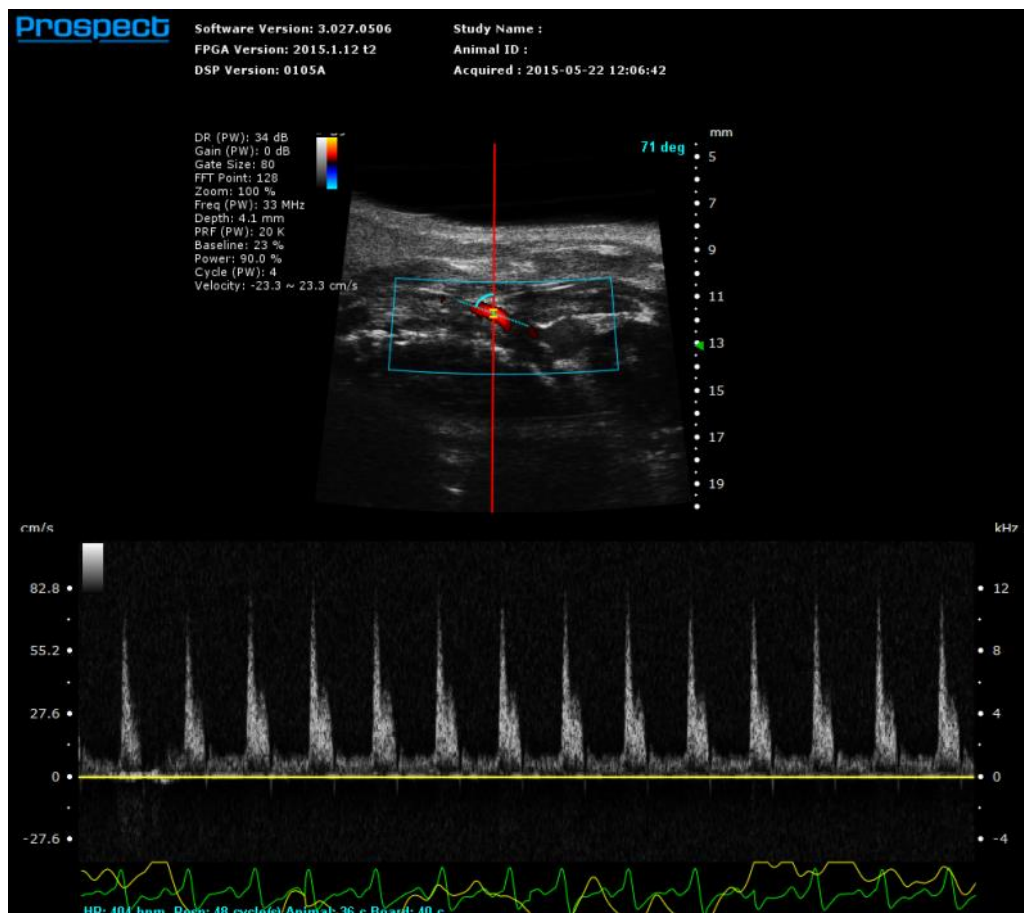
Fig. 32. Configuration of operation showing how to image the LCCA in the left parasternal longitudinal section. (A) Long hinge position from the anterior view. (B) Short hinge position from the inferior view. (C) Transducer position.



(A)



(B)



(C)

Fig. 33. LCCA imaging of the mouse: (A) B-mode image showing the LCCA in its longitudinal section and the AAr in its cross section. (B) color Doppler-mode image, and (C) PW-mode image.

References

1. J. G. Fox, S. W. Barthold, M. T. Davisson, C. E. Newcomer, F. W. Quimby and A. L. Smith, “The Mouse in Biomedical Research”, *Elsevier*, 2007.
2. H. J. Hedrich, “The Laboratory Mouse”, *Elsevier*, 2012.
3. Y. Q. Zhou, F. S. Foster, B. J. Nieman, L. Davidson, X. J. Chen and R. M. Henkelman, “Comprehensive transthoracic cardiac imaging in mice using ultrasound biomicroscopy with anatomical confirmation by magnetic resonance imaging”, *Physiological Genomics*, 18, P. 232–244, 2004.
4. X. P. Yang, Y. H. Liu, N. E. Rhaleb, N. Kurihara, H. E. Kim, and O. A. Carretero, “Echocardiographic assessment of cardiac function in conscious and anesthetized mice”, *American Journal of Physiology-Heart and Circulatory Physiology*, 277, P. H1967-H1974, 1999.
5. M. Vinhas, A. C. Araújo, S. Ribeiro, L. B. Rosário and J. A. Belo, “Transthoracic echocardiography reference values in juvenile and adult 129/Sv mice”, *BioMed Central Cardiovascular Ultrasound*, 11:12, 2013.

Appendix A

Cardiac indices measurements

In PROSPECT High Resolution Imaging System, the physical parameter measurements for cardiac applications are provided, and many cardiac indices are available such as fractional shortening (FS), ejection fraction (EF), stroke volume (SV), cardiac output (CO) and so on. The detailed operational steps of these cardiac indices measurements are described as follows:

To get the cardiac parameters:

1. Click the desired measurements on the cardiac package list.

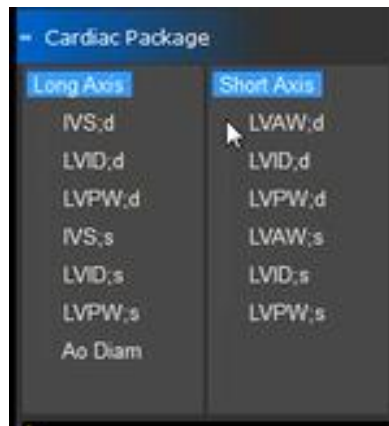


Fig. A1. Cardiac package list

2. Click on the image to place the start and end points.

Note: Because such as RVAW;d → RVID;d → IVS;d → LVID;d → LVPW;d or LVAW;s → LVID;s → LVPW;s are continuously measurements, it can automatically start the next measurement until finishing LVPW;d/LVPW;s. It means the pervious one's end point is the next one's start point.

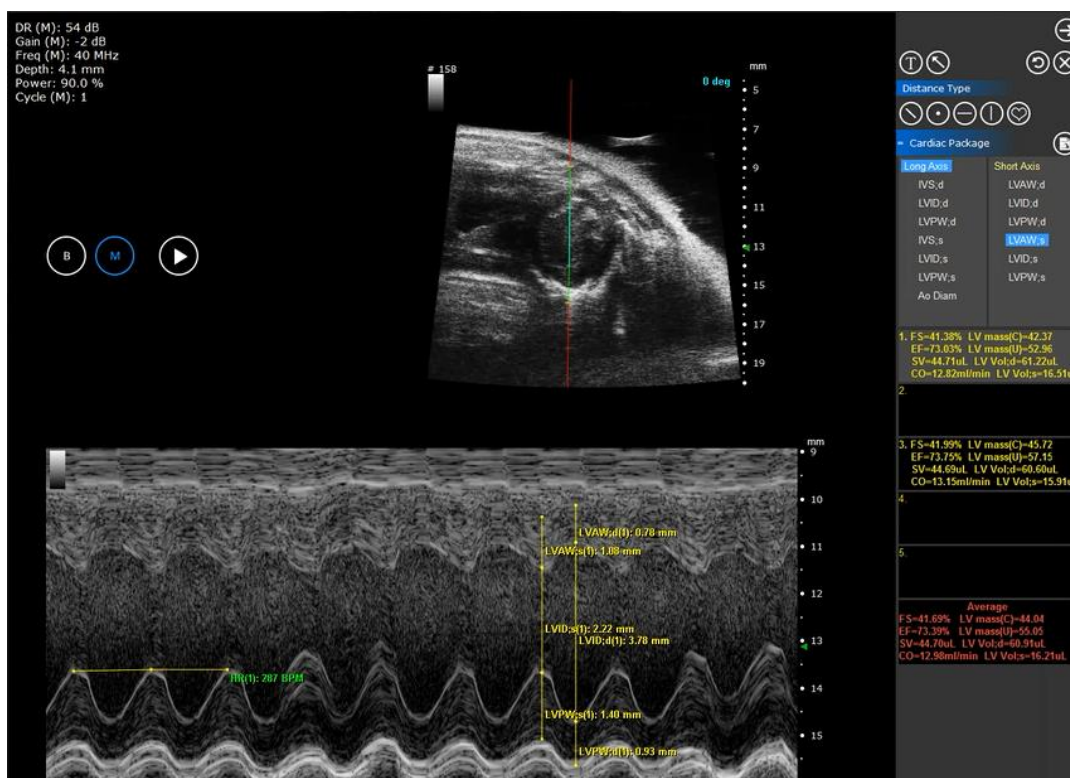


Fig. A2. Cardiac package measurements.

3. After completing desired measurements, click  to export the cardiac indices in CSV-format file. In the report, the cardiac index will be calculated if it has enough parameters (see Table A1). And the average and standard deviation of every measurement and calculation are also calculated.

Note: if there is not existed the measurement or the calculation have not enough parameters, "N/A" is showed on the report.

Table A1 Cardiac indices with corresponding required parameters

| Calculation | Required parameters |
|-----------------------|-----------------------|
| LVFS | LVID;d, LVID;s |
| RVFS | RVID;d, RVID;s |
| IVSd/LVPWd | IVS;d, LVPW;d |
| IVSs/LVPWs | IVS;s, LVPW;s |
| LV Vol;d | LVID;d |
| LV Vol;s | LVID;s |
| RV Vol;d | RVID;d |
| RV Vol;s | RVID;s |
| LVEF | LVID;d, LVID;s |
| RVEF | RVID;d, RVID;s |
| PWTH | LVPW;d, LVPW;s |
| LV mass (Corrected) | LVID;d, LVPW;d, IVS;d |
| LV mass (Uncorrected) | LVID;d, LVPW;d, IVS;d |
| RWT;d | LVPW;d, LVID;s |
| RWT;s | LVPW;s, LVID;d |
| SV | LVID;d, LVID;s, HR |
| CO | LVID;d, LVID;s |

| | A | B | C | D | E | F | G |
|----|-----------------------|---------------|---------|---------|---------|-----|---|
| 5 | Study name | Tumor | | | | | |
| 6 | Animal ID | Mouse 1 | | | | | |
| 7 | Series name | Series 1 | | | | | |
| 8 | Image label | Image Level 1 | | | | | |
| 9 | | | | | | | |
| 10 | Measurement | Type | Units | Value 1 | Average | STD | |
| 11 | HR | Heart Rate | BPM | 337.01 | 337.01 | 0 | |
| 12 | RVAWd | Depth | mm | N/A | N/A | N/A | |
| 13 | RVIDd | Depth | mm | N/A | N/A | N/A | |
| 14 | IVSd | Depth | mm | 1.08 | 1.08 | 0 | |
| 15 | LVIDd | Depth | mm | 3.56 | 3.56 | 0 | |
| 16 | LVPWd | Depth | mm | 0.78 | 0.78 | 0 | |
| 17 | RVAWs | Depth | mm | N/A | N/A | N/A | |
| 18 | RVIDs | Depth | mm | N/A | N/A | N/A | |
| 19 | IVSs | Depth | mm | 1.65 | 1.65 | 0 | |
| 20 | LVIDs | Depth | mm | 2.24 | 2.24 | 0 | |
| 21 | LVPWs | Depth | mm | 1.23 | 1.23 | 0 | |
| 22 | LVAWd | Depth | mm | N/A | N/A | N/A | |
| 23 | LVAWs | Depth | mm | N/A | N/A | N/A | |
| 24 | Ao Diam | Depth | mm | N/A | N/A | N/A | |
| 25 | | | | | | | |
| 26 | Calculation | Units | Value 1 | Average | STD | | |
| 27 | LVFS | % | 36.97 | 36.97 | 0 | | |
| 28 | RVFS | % | N/A | N/A | N/A | | |
| 29 | IVSd/LVPWd | | 1.38 | 1.38 | 0 | | |
| 30 | IVSs/LVPWs | | 1.34 | 1.34 | 0 | | |
| 31 | LV Vol;d | microL | 53.03 | 53.03 | 0 | | |
| 32 | LV Vol;s | microL | 17.04 | 17.04 | 0 | | |
| 33 | RV Vol;d | microL | N/A | N/A | N/A | | |
| 34 | RV Vol;s | microL | N/A | N/A | N/A | | |
| 35 | LVEF | % | 67.87 | 67.87 | 0 | | |
| 36 | RVEF | % | N/A | N/A | N/A | | |
| 37 | PWTH | % | 57.69 | 57.69 | 0 | | |
| 38 | LV mass (Corrected) | mg | 95.56 | 95.56 | 0 | | |
| 39 | LV mass (Uncorrected) | mg | 119.44 | 119.44 | 0 | | |
| 40 | RWT;d | | 0.35 | 0.35 | 0 | | |
| 41 | RWT;s | | 0.34 | 0.34 | 0 | | |
| 42 | SV | microL | 35.99 | 35.99 | 0 | | |
| 43 | CO | mL/min | 12.13 | 12.13 | 0 | | |

Fig. A3. The report of cardiac package measurements.

Appendix B

The reference value of the cardiac parameters

Table 1. The effect of anesthesia on heart rate, ventricular wall thickness, and chamber dimensions in Twelve-week-old male 129 SvEv/Tac mice weighing 23–28g. [4]

| Group | n | BW, g | HR, beats/min | Systolic Dimensions, mm | | | Diastolic Dimensions, mm | | |
|---------------------|----|------------|---------------|-------------------------|--------------|--------------|--------------------------|--------------|--------------|
| | | | | IVST | LVD | PWT | IVST | LVD | PWT |
| Conscious | 24 | 24.0 ± 0.4 | 658 ± 9 | 0.90 ± 0.02 | 1.22 ± 0.05 | 0.95 ± 0.02 | 0.56 ± 0.01 | 2.52 ± 0.06 | 0.62 ± 0.06 |
| Pentobarbital | 12 | 23.7 ± 0.4 | 377 ± 11† | 0.81 ± 0.01† | 2.05 ± 0.08† | 0.85 ± 0.02* | 0.54 ± 0.01 | 3.06 ± 0.09† | 0.57 ± 0.02* |
| Ketamine + xylazine | 12 | 24.3 ± 0.6 | 293 ± 19† | 0.91 ± 0.02 | 2.34 ± 0.08† | 0.89 ± 0.03 | 0.43 ± 0.01† | 3.57 ± 0.09† | 0.42 ± 0.01† |

Values are means ± SE; n = no. of mice. BW, body weight; HR, heart rate; IVST, interventricular septal thickness; LVD, left ventricular dimension; PWT, posterior wall thickness. *P < 0.01; †P < 0.001 vs. conscious mice.

The following data was obtained from 30 wild type male 129/Sv mice (Harlan Laboratories) which were divided by two groups, 15 juvenile mice (3 weeks) and 15 adult mice (8 weeks). [5]

Table 2. Echocardiographic measurements from B-mode images

| Measurement | Juvenile | n | Adult | n | p |
|-----------------------------|---------------|----|--------------|----|---------|
| LVEndoLd (mm) | 6.18 (0.57) | 15 | 7.40 (0.58) | 15 | < 0.001 |
| LVEndoLs (mm) | 4.99 ± 0.38 | 15 | 6.58 ± 0.45 | 15 | < 0.001 |
| LVEpiLd (mm) | 6.38 (0.56) | 15 | 7.65 (0.67) | 15 | < 0.001 |
| LVEpiLs (mm) | 5.35 ± 0.34 | 15 | 7.03 ± 0.44 | 15 | < 0.001 |
| LVEndoAd (mm ²) | 6.06 ± 0.87 | 15 | 9.87 ± 1.20 | 15 | < 0.001 |
| LVEndoAs (mm ²) | 3.06 (0.98) | 15 | 4.25 (1.12) | 15 | < 0.001 |
| LVEpiAd (mm ²) | 11.85 ± 1.73 | 15 | 19.47 ± 1.71 | 15 | < 0.001 |
| LVEpiAs (mm ²) | 8.84 ± 1.83 | 15 | 14.46 ± 1.57 | 15 | < 0.001 |
| EAC (mm ²) | 3.22 ± 0.81 | 15 | 5.62 ± 1.16 | 15 | < 0.001 |
| FAC (%) | 52.89 ± 10.07 | 15 | 56.87 ± 7.80 | 15 | ns |
| LWvd (μl) | 29.57 ± 6.04 | 15 | 59.90 ± 8.78 | 15 | < 0.001 |
| LWVs (μl) | 11.85 ± 3.19 | 15 | 23.32 ± 5.31 | 15 | < 0.001 |
| LVM (mg) | 39.68 ± 8.64 | 15 | 81.90 ± 9.69 | 15 | < 0.001 |
| LVMi (mg/g) | 5.26 ± 1.27 | 15 | 4.16 ± 0.42 | 15 | 0.005 |
| AoD (mm) | 0.93 ± 0.09 | 15 | 1.27 ± 0.13 | 15 | < 0.001 |
| PAD (mm) | 1.34 ± 0.11 | 15 | 1.59 ± 0.13 | 15 | < 0.001 |

Values are mean ± SD or median (IQR), as appropriate. p = statistical significance; ns = not significant. n = 15 for all measurements.

LVEndoL = Left ventricle endocardial length. LVEpiL = Left ventricle epicardial length. LVEndoA = Left ventricle endocardial area. LVEpiA = Left ventricle epicardial area. EAC = Endocardial area change. FAC = Fractional area change. LWV = Left ventricle volume. LVM = Left ventricle mass. LVMi = LVM index. AoD = Ascending aorta diameter. PAD = Pulmonary artery diameter. -d = In diastole. -s = In systole.

Table 3. Echocardiographic measurements from M-mode images

| Measurement | Juvenile | n | Adult | n | p |
|-------------|--------------|----|--------------|----|---------|
| LVAWd (mm) | 0.61 ± 0.09 | 15 | 0.74 ± 0.14 | 15 | 0.005 |
| LVAWs (mm) | 0.85 ± 0.13 | 15 | 1.08 ± 0.18 | 15 | < 0.001 |
| LVIDd (mm) | 2.84 ± 0.20 | 15 | 3.56 ± 0.19 | 15 | < 0.001 |
| LVIDs (mm) | 1.96 ± 0.21 | 15 | 2.44 ± 0.28 | 15 | < 0.001 |
| LVPWd (mm) | 0.59 ± 0.15 | 15 | 0.64 ± 0.13 | 15 | ns |
| LVPWs (mm) | 0.81 ± 0.17 | 15 | 0.88 ± 0.19 | 15 | ns |
| EF (%) | 59.63 ± 9.05 | 15 | 59.91 ± 8.15 | 15 | ns |
| FS (%) | 30.76 ± 6.15 | 15 | 31.45 ± 5.63 | 15 | ns |
| IVSd (mm) | 0.41 ± 0.08 | 15 | 0.47 ± 0.15 | 15 | ns |
| IVSs (mm) | 0.50 ± 0.13 | 15 | 0.62 ± 0.25 | 15 | ns |
| RVIDd (mm) | 1.08 ± 0.15 | 7 | 1.42 ± 0.19 | 11 | 0.001 |
| RVIDs (mm) | 0.65 (0.31) | 7 | 0.89 (0.21) | 11 | ns |
| RVAWd (mm) | 0.50 ± 0.11 | 7 | 0.32 ± 0.08 | 11 | 0.001 |
| RVAWs (mm) | 0.66 ± 0.16 | 7 | 0.57 ± 0.13 | 11 | ns |

Values are mean ± SD or median (IQR), as appropriate. p = statistical significance. ns = not significant. n = 15 for all measurements, except for RV measurements (n = 7 for the juveniles and n = 11 for the adults). LVAW = Left ventricle anterior wall. LVID = Left ventricle internal diameter. LVPW = Left ventricle posterior wall. EF = Ejection fraction. FS = Fractional shortening. IVS = Interventricular septum. RVID = Right ventricle internal diameter. RVAW = Right ventricle anterior wall. -d = In diastole. -s = In systole.

Table 4. Echocardiographic measurements from Doppler images

| Measurement | Juvenile | n | Adult | n | p |
|----------------|------------------|----|------------------|----|---------|
| AoVPPV (mm/s) | 1055.28 (327.21) | 15 | 1557.67 (693.61) | 15 | 0.003 |
| AET (ms) | 50.37 ± 4.56 | 15 | 49.59 ± 4.50 | 15 | ns |
| AoVPPG (mmHg) | 4.45 (3.13) | 15 | 9.76 (9.46) | 15 | 0.003 |
| DAoPV (mm/s) | 747.59 (162.89) | 15 | 1049.88 (321.15) | 15 | 0.002 |
| SV (μl) | 31.93 ± 8.67 | 15 | 70.61 ± 24.66 | 15 | < 0.001 |
| CO (ml/min) | 12.06 ± 4.05 | 15 | 29.71 ± 10.13 | 15 | < 0.001 |
| COi (ml/min.g) | 1.54 ± 0.36 | 15 | 1.48 ± 0.39 | 15 | ns |
| PVPV (mm/s) | 663.34 ± 141.08 | 15 | 810.62 ± 149.55 | 15 | 0.01 |
| PVPPG (mmHg) | 1.83 ± 0.77 | 15 | 2.71 ± 0.96 | 15 | 0.01 |
| MVE (mm/s) | 673.53 ± 149.31 | 15 | 747.08 ± 92.31 | 15 | ns |
| MVA (mm/s) | 456.51 ± 73.29 | 15 | 500.17 ± 85.14 | 15 | ns |
| IVCT (ms) | 10.90 ± 2.76 | 15 | 12.91 ± 3.45 | 15 | ns |
| IVRT (ms) | 16.52 ± 3.29 | 15 | 12.48 ± 2.49 | 15 | 0.001 |
| MVET (ms) | 61.05 ± 9.74 | 15 | 59.24 ± 8.34 | 15 | ns |
| NFT (ms) | 77.45 ± 5.66 | 15 | 75.66 ± 7.57 | 15 | ns |
| MVPPG (mmHg) | 1.98 ± 0.76 | 15 | 2.30 ± 0.52 | 15 | ns |
| MVE/A | 1.50 ± 0.37 | 15 | 1.53 ± 0.27 | 15 | ns |
| LVMPI | 0.55 ± 0.14 | 15 | 0.51 ± 0.07 | 15 | ns |
| TVE (mm/s) | 241.72 ± 30.57 | 12 | 252.83 ± 77.42 | 6 | ns |
| TVA (mm/s) | 400.90 ± 47.96 | 12 | 386.53 ± 123.06 | 6 | ns |
| TvPPG (mmHg) | 0.74 ± 0.21 | 12 | 0.68 ± 0.39 | 6 | ns |
| TVE/A | 0.60 ± 0.06 | 12 | 0.66 ± 0.13 | 6 | ns |

Values are mean ± SD or median (IQR), as appropriate. p = statistical significance. ns = not significant. n = 15 for all measurements, except for TV measurements (n = 12 for the juveniles and n = 6 for the adults).

AoVPPV = Ascending aorta valve peak velocity. AET = Aortic ejection time. AoVPPG = Ascending aorta valve peak pressure gradient. DAoPV = Descending aorta peak velocity. SV = Stroke volume. CO = Cardiac output. COi = CO index. PVPV = Pulmonary valve peak velocity. PVPPG = Pulmonary valve peak pressure gradient. MVE = Mitral valve early wave peak. MVA = Mitral valve atrial wave peak. IVCT = Isovolumic contraction time. IVRT = Isovolumic relaxation time. MVET = Mitral valve ejection time. NFT = No Flow Time. MVPPG = Mitral valve peak pressure gradient. LVMPI = Left ventricle myocardial performance index. TVE = Tricuspid valve early wave peak. TVA = Tricuspid valve atrial wave peak. TvPPG = Tricuspid valve peak pressure gradient.